

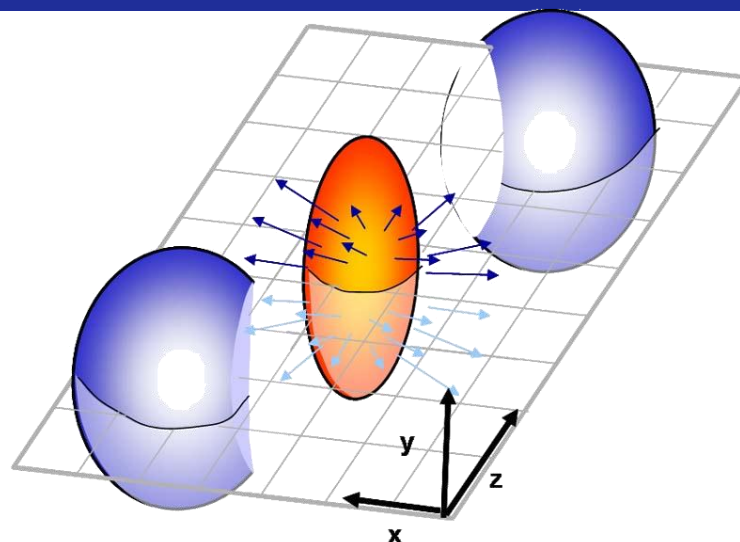


ATLAS flow measurements

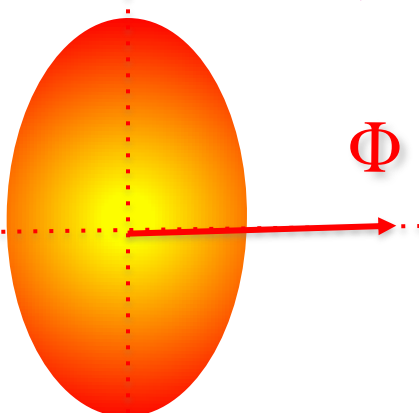
Jiangyong Jia for the ATLAS Collaboration

HPT2012 Oct 21th- Oct 24th

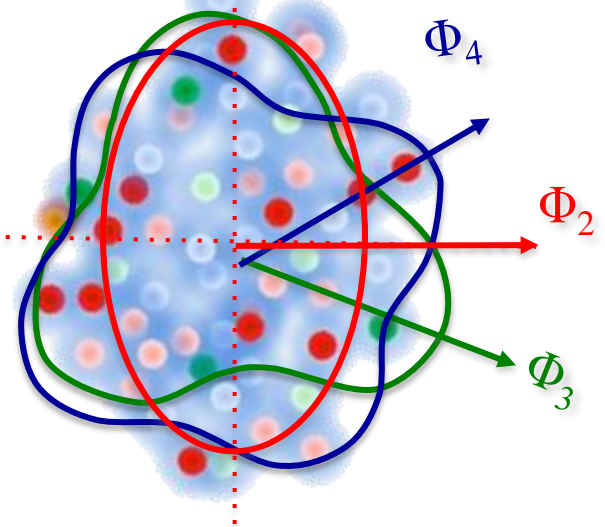
Initial geometry to azimuthal anisotropy



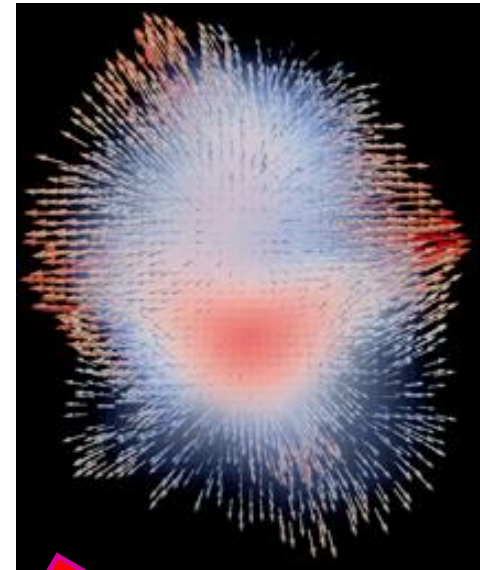
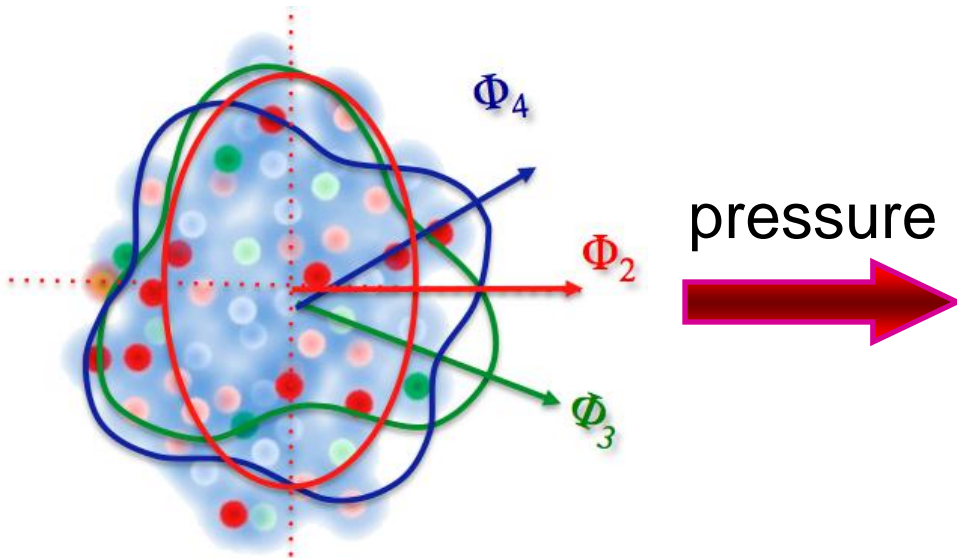
Simplified



Realistic



Initial geometry to azimuthal anisotropy



by MADAI.us

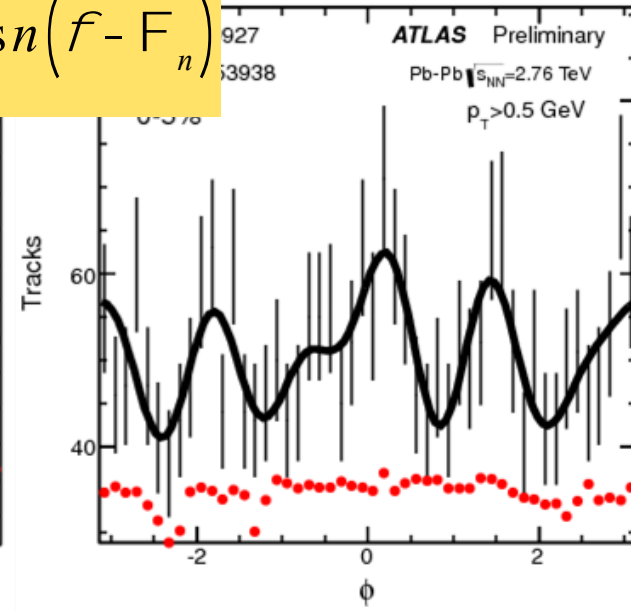
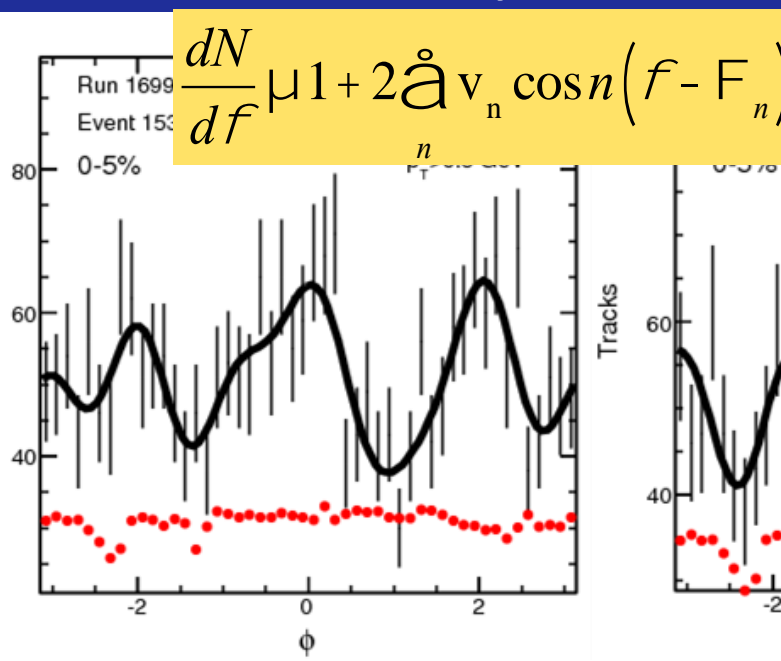
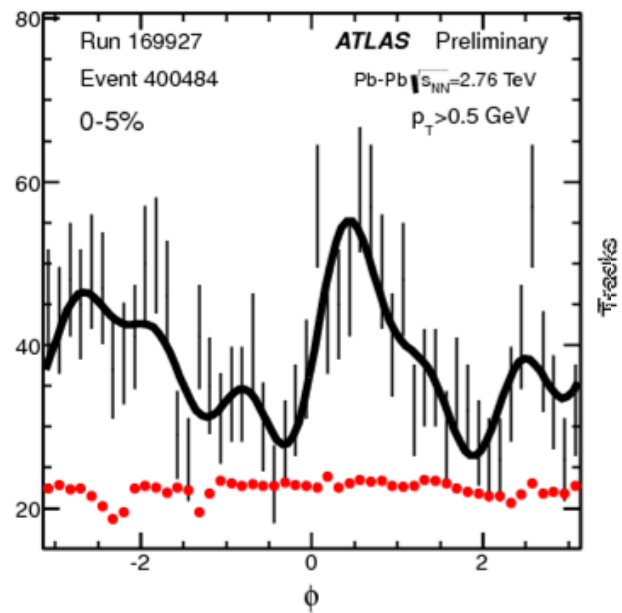
Single particle distribution

$$\frac{dN}{df} \propto 1 + 2\sum_n \langle v_n^a v_n^b \cos(n(\phi - \phi_n)) \rangle$$

Pair distribution

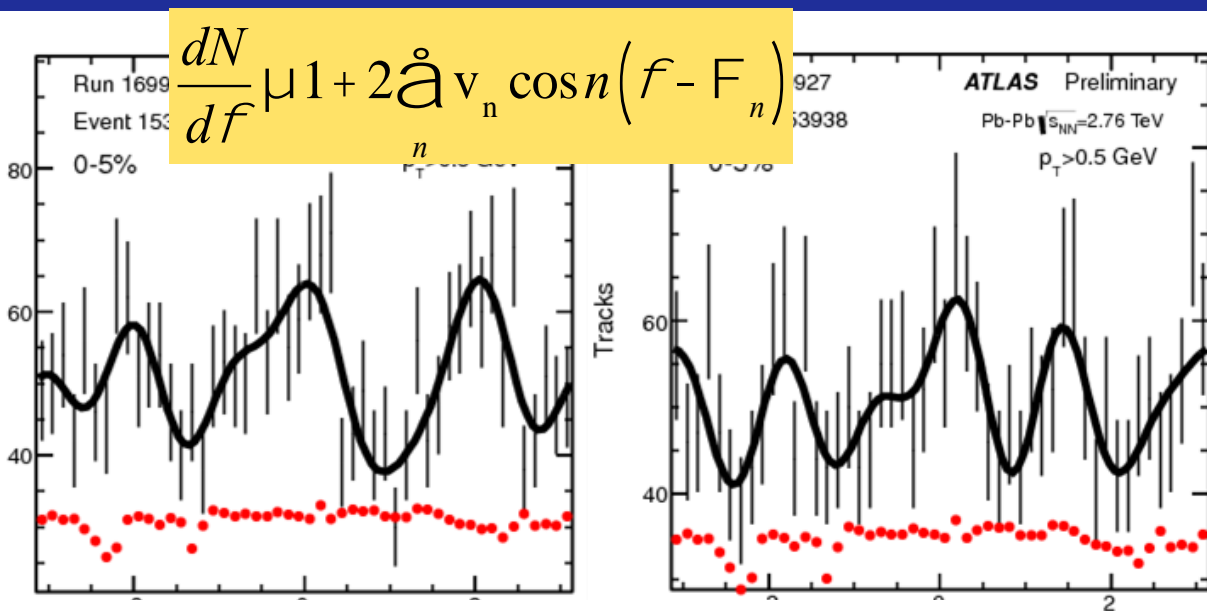
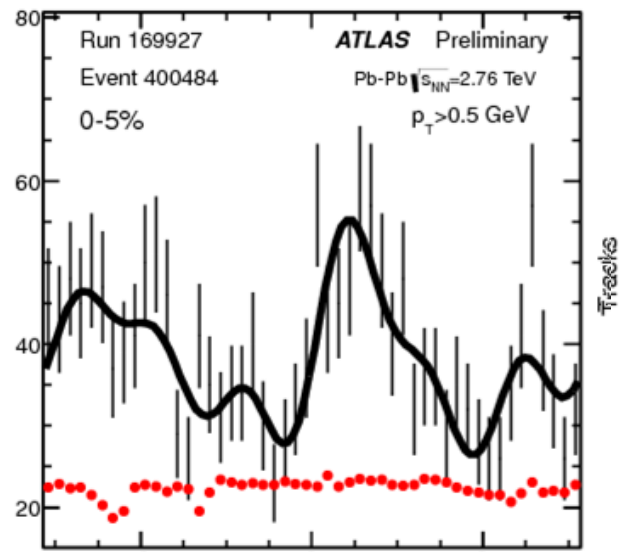
$$\frac{dN}{dDf} = \left[\frac{dN}{df_a} * \frac{dN}{df_b} \right] \propto 1 + \sum_n 2v_n^a v_n^b \cos(nDf)$$

Fluctuation event by event

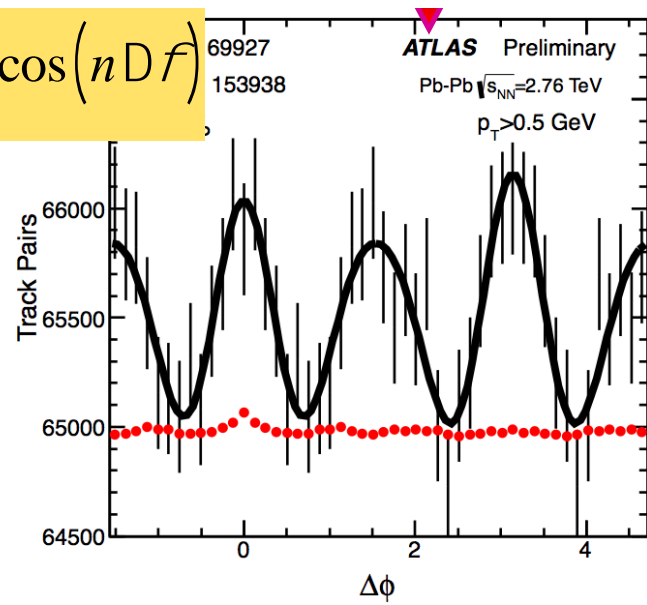
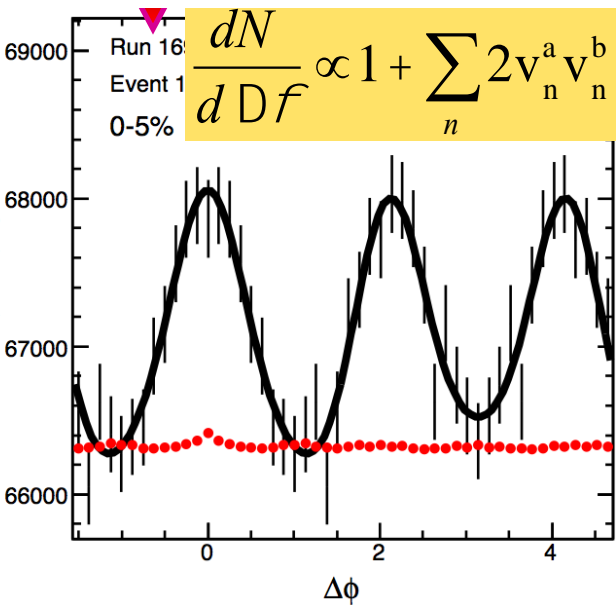
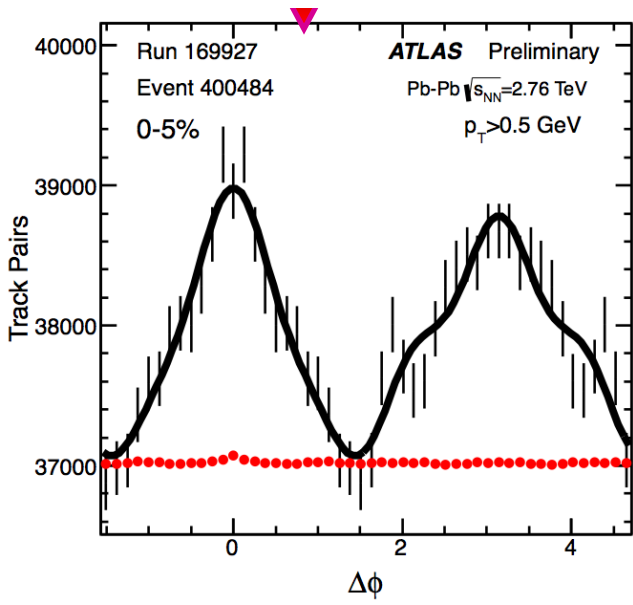


- Significant fluctuations, factor of ~ 2 in central events
- Can not be explained by detector effects (red histogram)

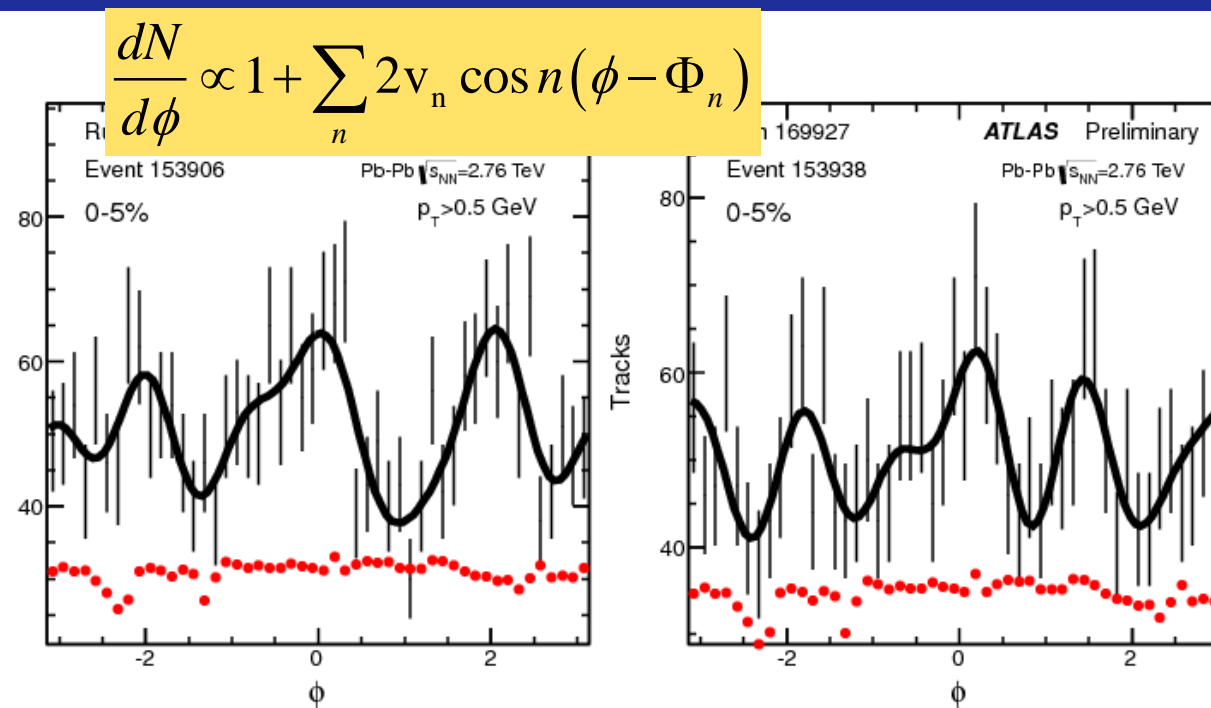
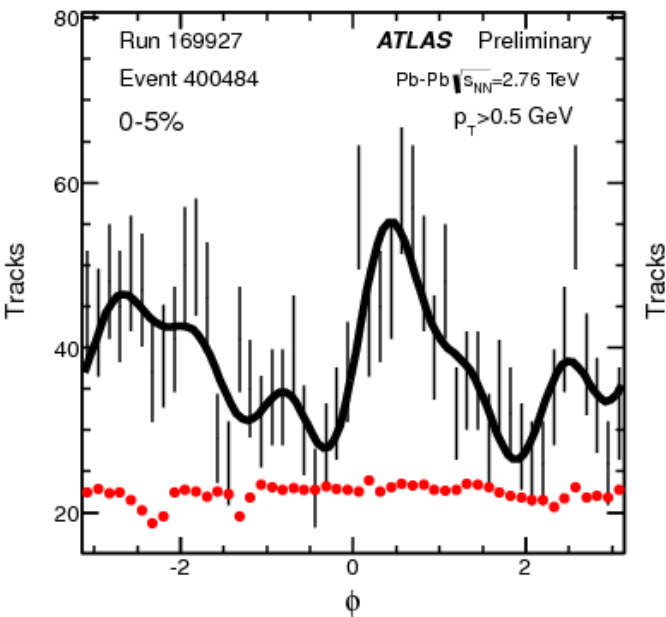
Fluctuation event by event



Rich event-by-event patterns for v_n and Φ_n !

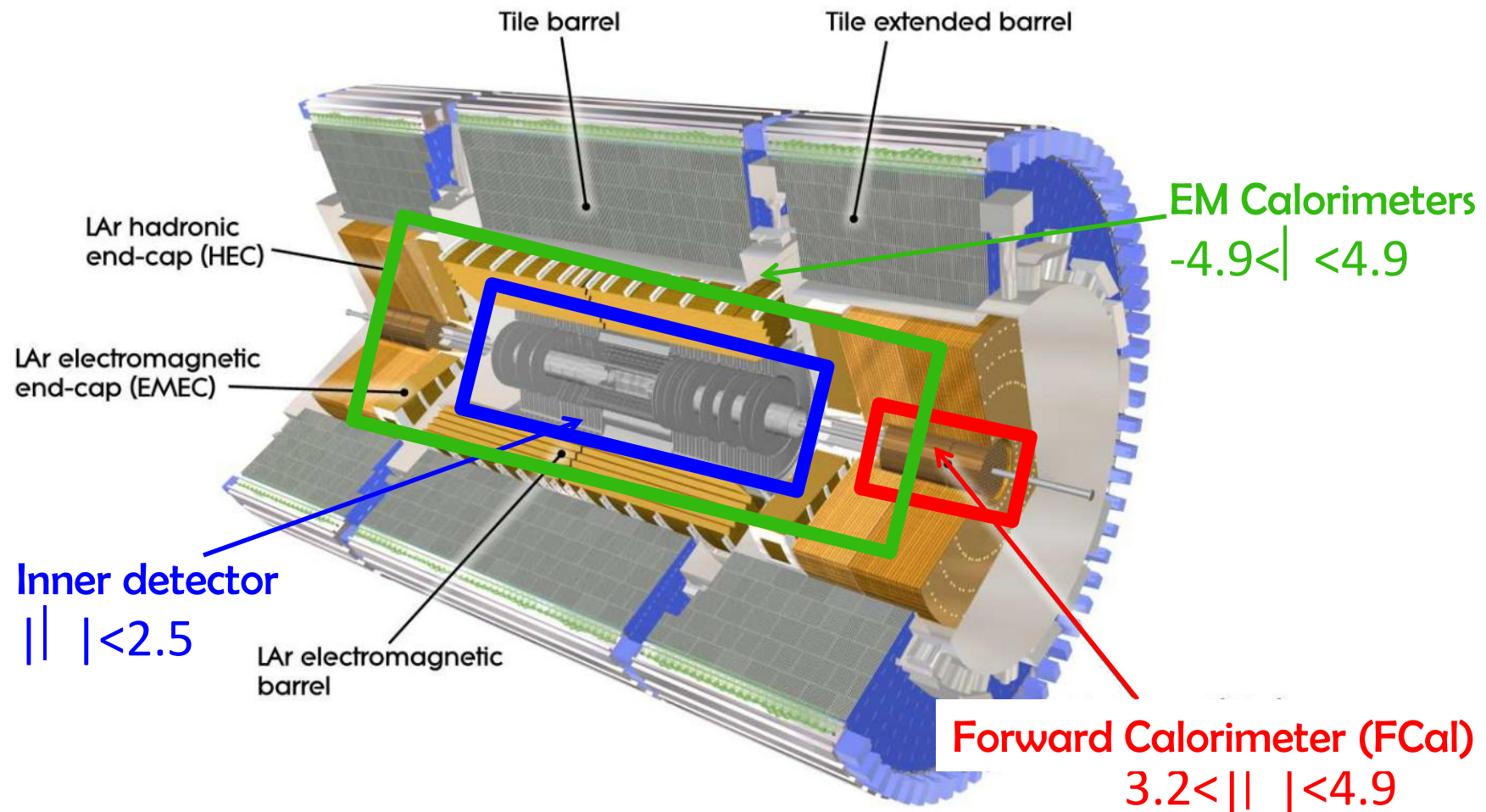


Flow observables



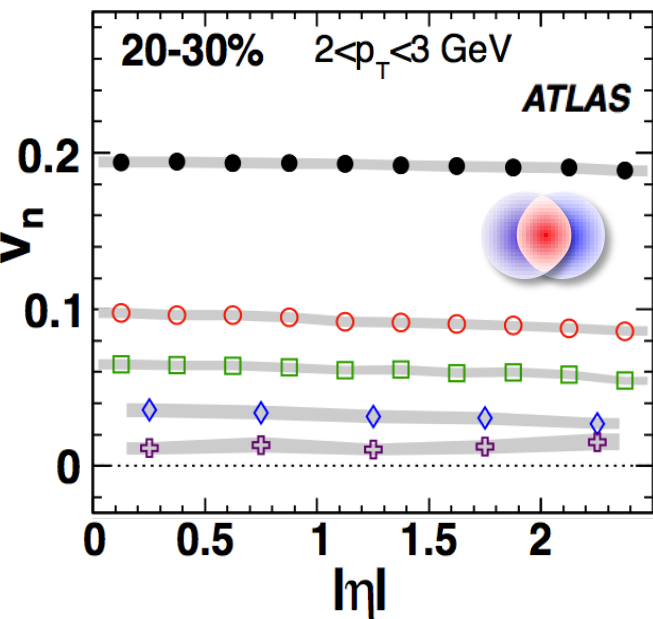
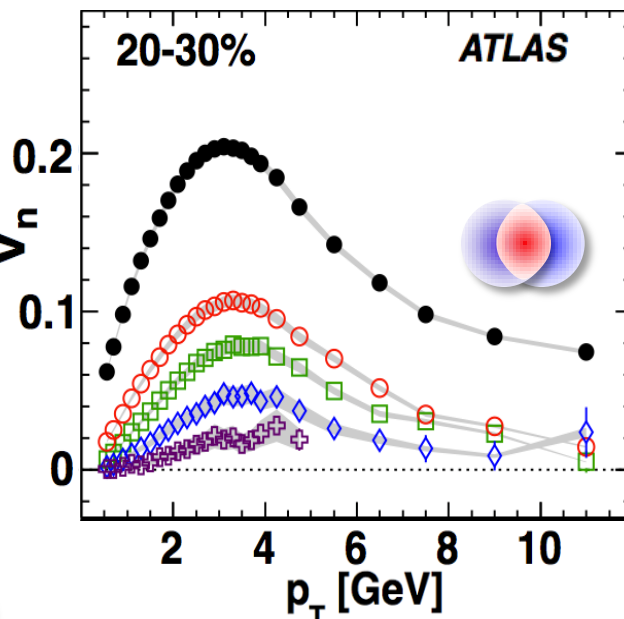
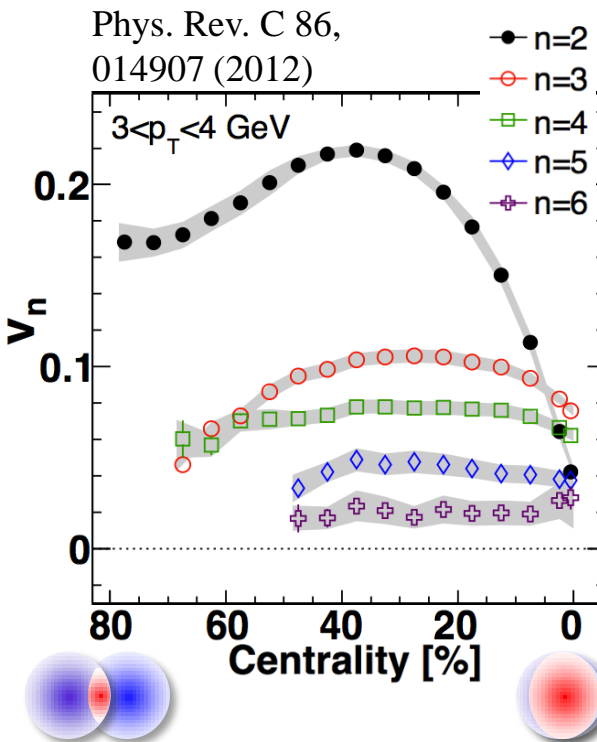
- Mean values of $v_n(p_T, \eta, \text{cent})$. PhysRevC.86.014907
- Event by event v_n distributions. ATLAS-CONF-2012-114
- Correlations between flow phases Φ_n . ATLAS-CONF-2012-49
- Probes into dynamical expansion of the matter
- Sensitive to the initial density distribution/fluctuations
- Extraction of the matter properties in more details

ATLAS detector



- Tracking $\parallel | < 2.5 \rightarrow$ for v_n measurement
- E_T in forward calorimeter $3.2 < |\eta| < 4.9 \rightarrow$ event plane
- Event plane correlations use entire calorimeter $-4.9 < |\eta| < 4.9$

Averaged flow: $v_n(\text{cent}, p_T, \eta)$

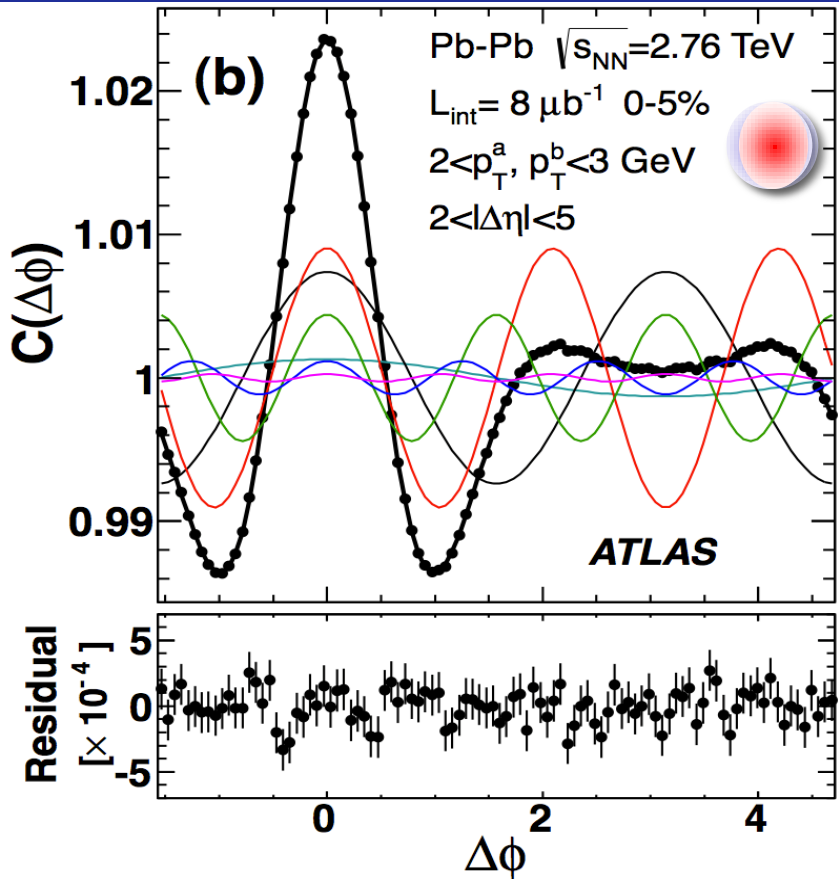
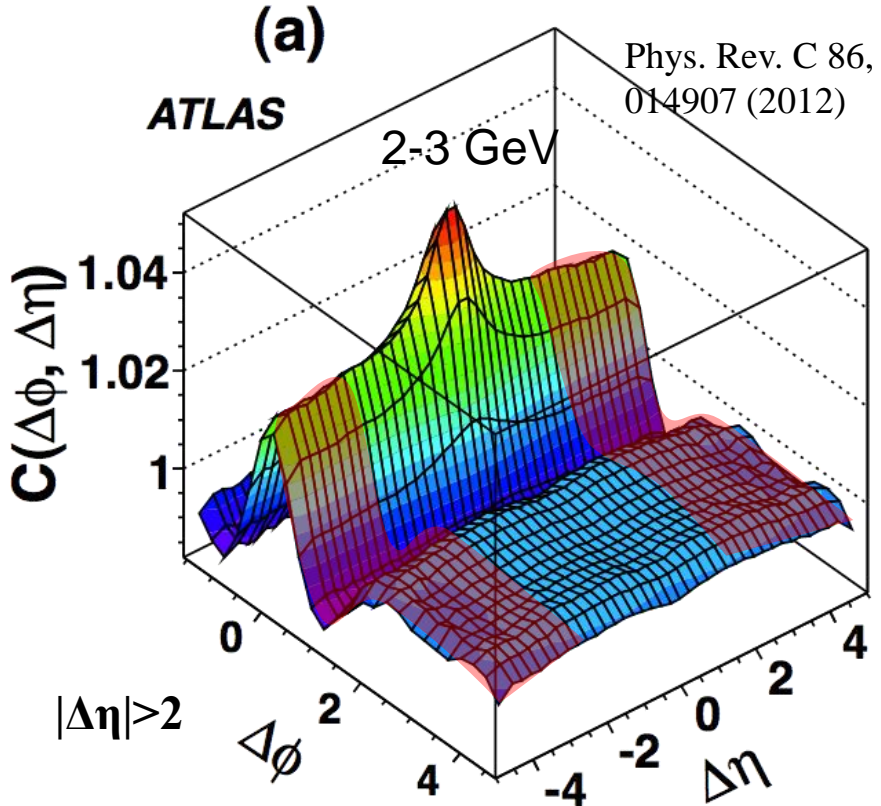


- Features of Fourier coefficients

- v_n coefficients rise and fall with centrality.
- v_n coefficients rise and fall with p_T .
- v_n coefficients are \sim boost invariant.

Flow correlations are long range!

v_n extraction via two-particle correlations (2PC) ⁹

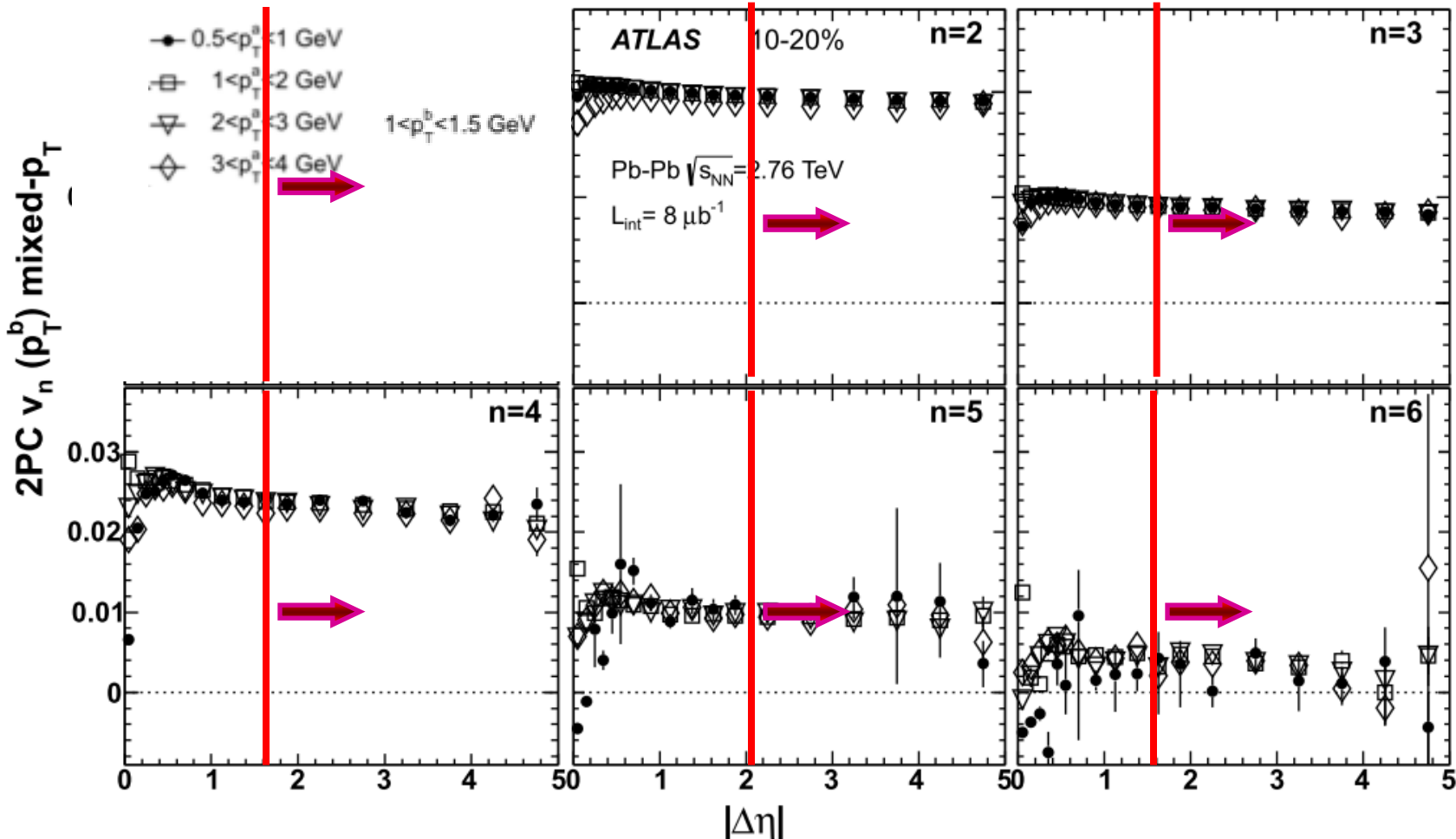


- Long range structures (“ridge”) described by harmonics $v_{1,1}-v_{6,6}$

$$\frac{dN}{dDf} \propto 1 + \sum_n 2v_{n,n}(p_T^a, p_T^b) \cos(nDf) \quad v_{n,n}(p_T^a, p_T^b) = v_n(p_T^a)v_n(p_T^b) + \text{non-flow}$$

Factorization of $v_{n,n}$ to v_n as a function of $\Delta\eta$

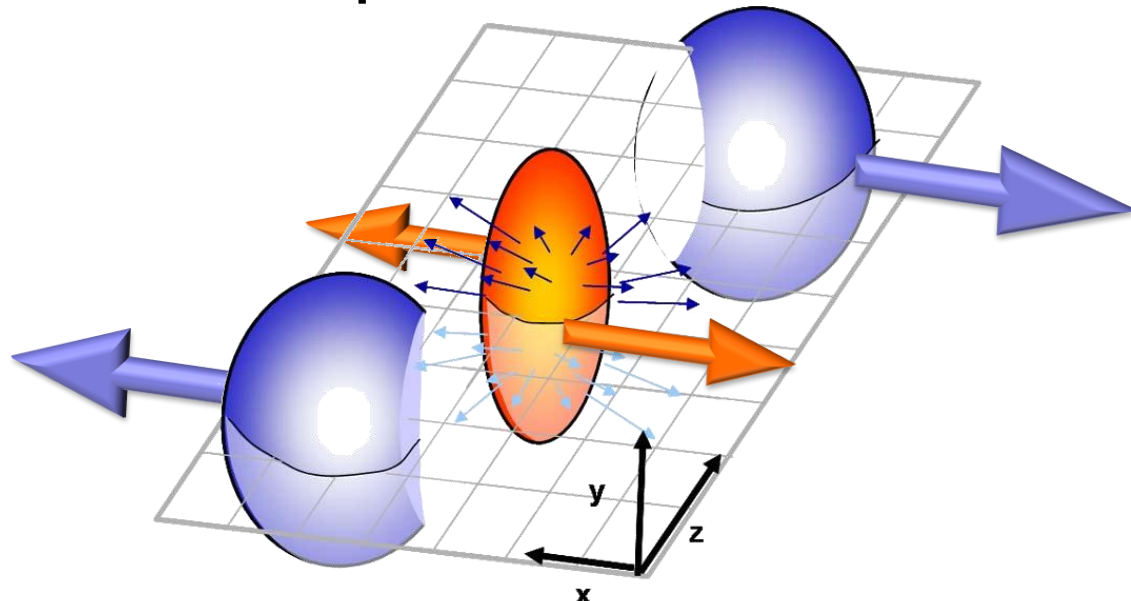
$$v_{n,n}(p_T^a, p_T^b) = v_n(p_T^a) \boxed{v_n(p_T^b)} + \text{non-flow}$$



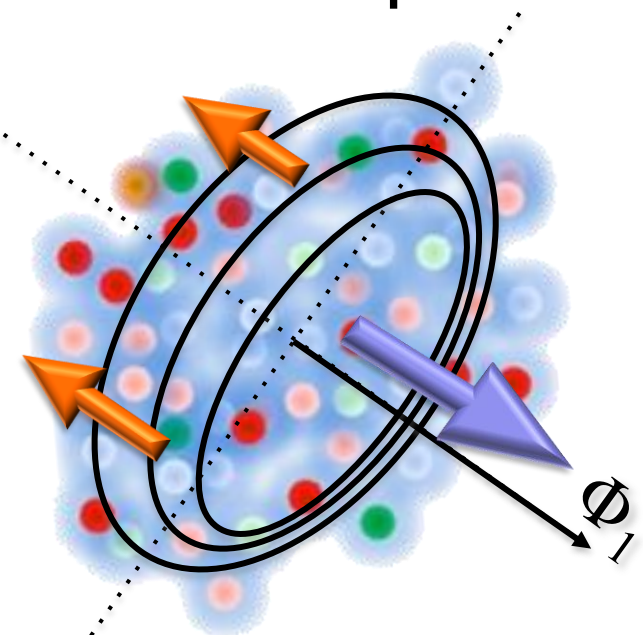
- Factorization works well for $n=2-6$, weak $\Delta\eta$ dependence
- Break down of $v_{1,1}$ is due to global momentum conservation

Dipolar flow v_1

Directed (odd component) flow vanishes at $\eta=0$



Dipolar (even component) flow ~boost invariant in η



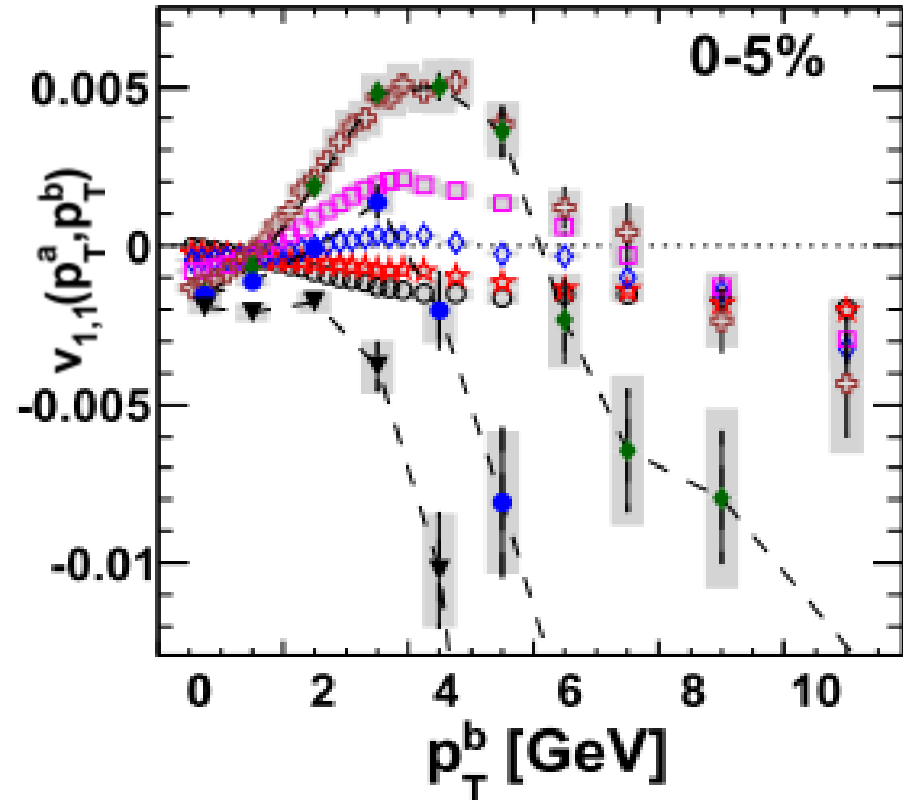
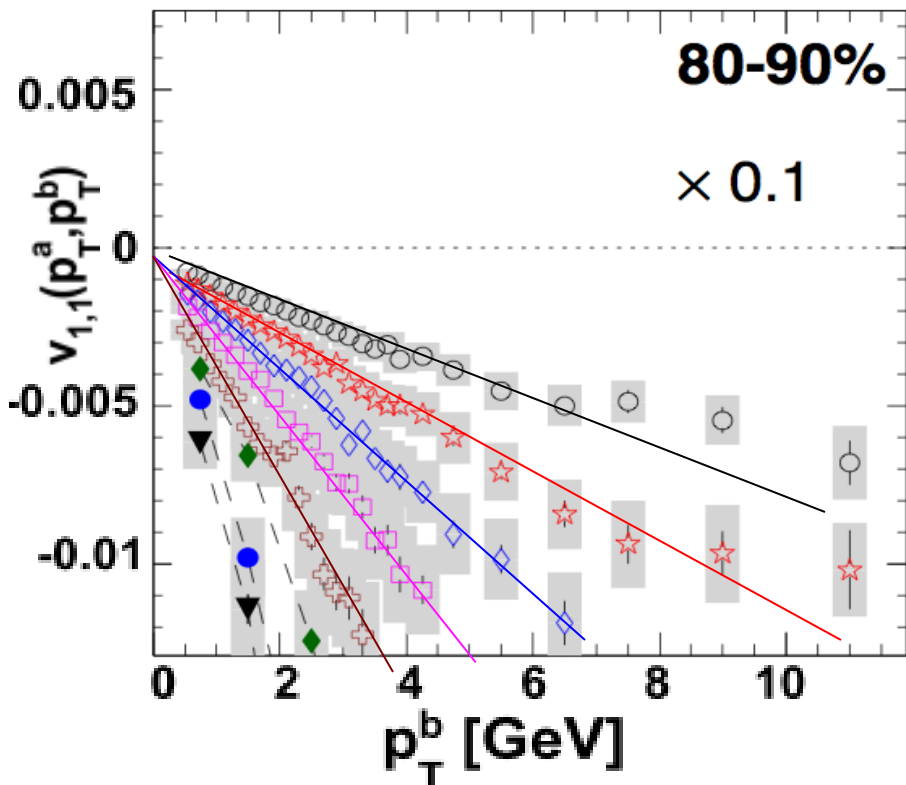
But also include non-flow effects: Momentum of individual particle must be balanced by others:

$$v_{1,1} \left(p_T^a, p_T^a \right) = v_1 \left(p_T^a \right) v_1 \left(p_T^b \right) + \text{non-flow} \approx - \frac{p_T^a \cdot p_T^b}{M \langle p_T^2 \rangle}$$

Behaviors of $v_{1,1}(p_T^a, p_T^b)$

○ $0.5 < p_T^a < 1 \text{ GeV}$
★ $1 < p_T^a < 1.5 \text{ GeV}$
◆ $3 < p_T^a < 4 \text{ GeV}$
◆ $4 < p_T^a < 6 \text{ GeV}$

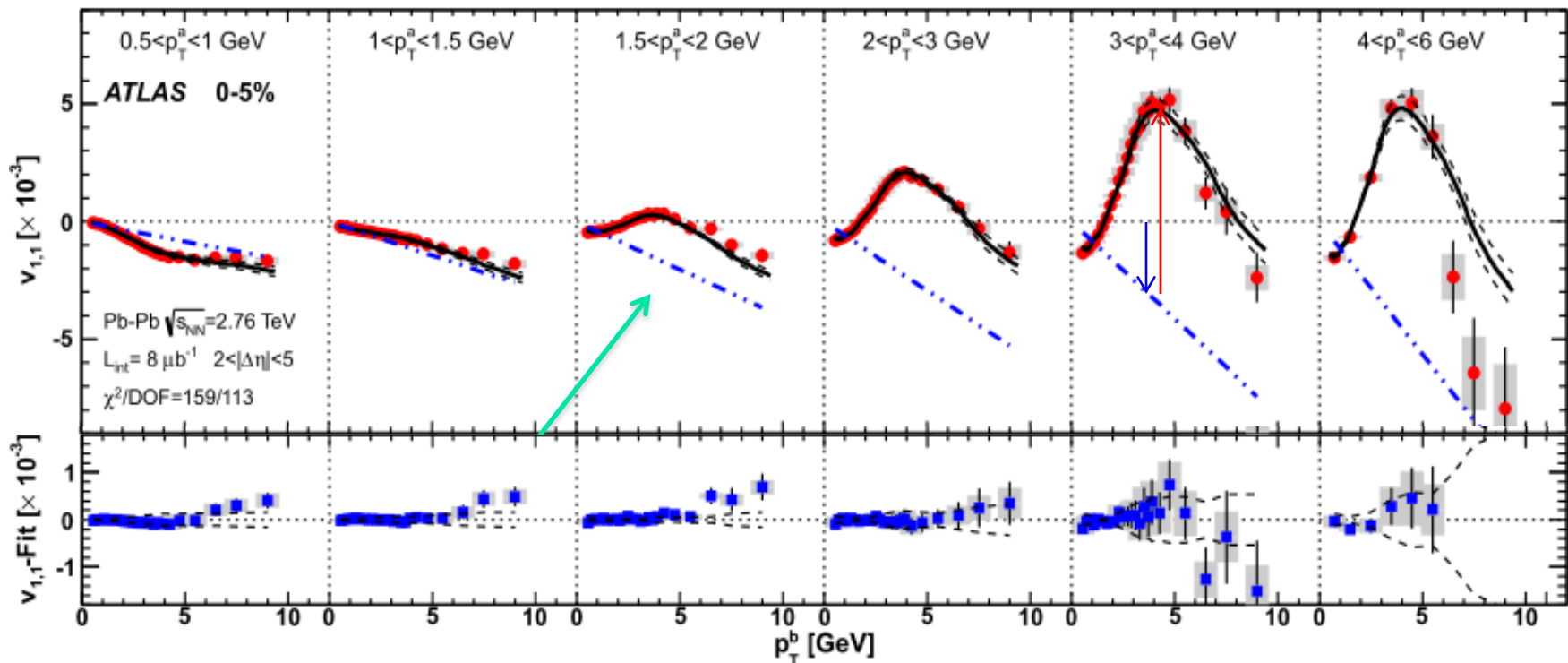
◇ $1.5 < p_T^a < 2 \text{ GeV}$
□ $2 < p_T^a < 3 \text{ GeV}$
● $6 < p_T^a < 8 \text{ GeV}$
▼ $8 < p_T^a < 20 \text{ GeV}$



Well described by
$$-\frac{p_T^a \times p_T^b}{M \langle p_T^2 \rangle}$$

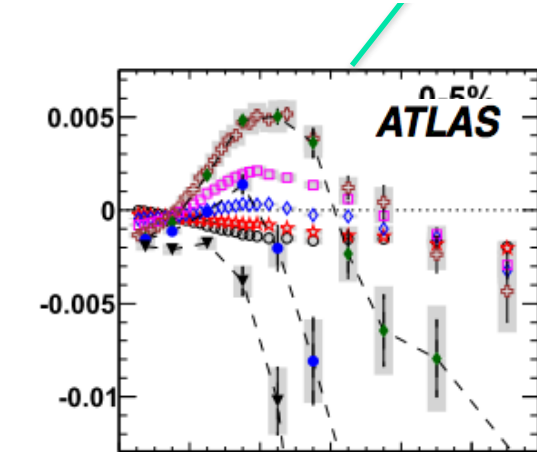
$$v_{1,1}(p_T^a, p_T^b) \stackrel{?}{=} v_1(p_T^a)v_1(p_T^b) - \frac{p_T^a \cdot p_T^b}{M \langle p_T^2 \rangle}$$

Extracting the | -even $v_1(p_T)$



$$v_{1,1}(p_T^a, p_T^b) = v_1^{\text{Fit}}(p_T^a)v_1^{\text{Fit}}(p_T^b) - cp_T^a p_T^b$$

Excellent Fit!



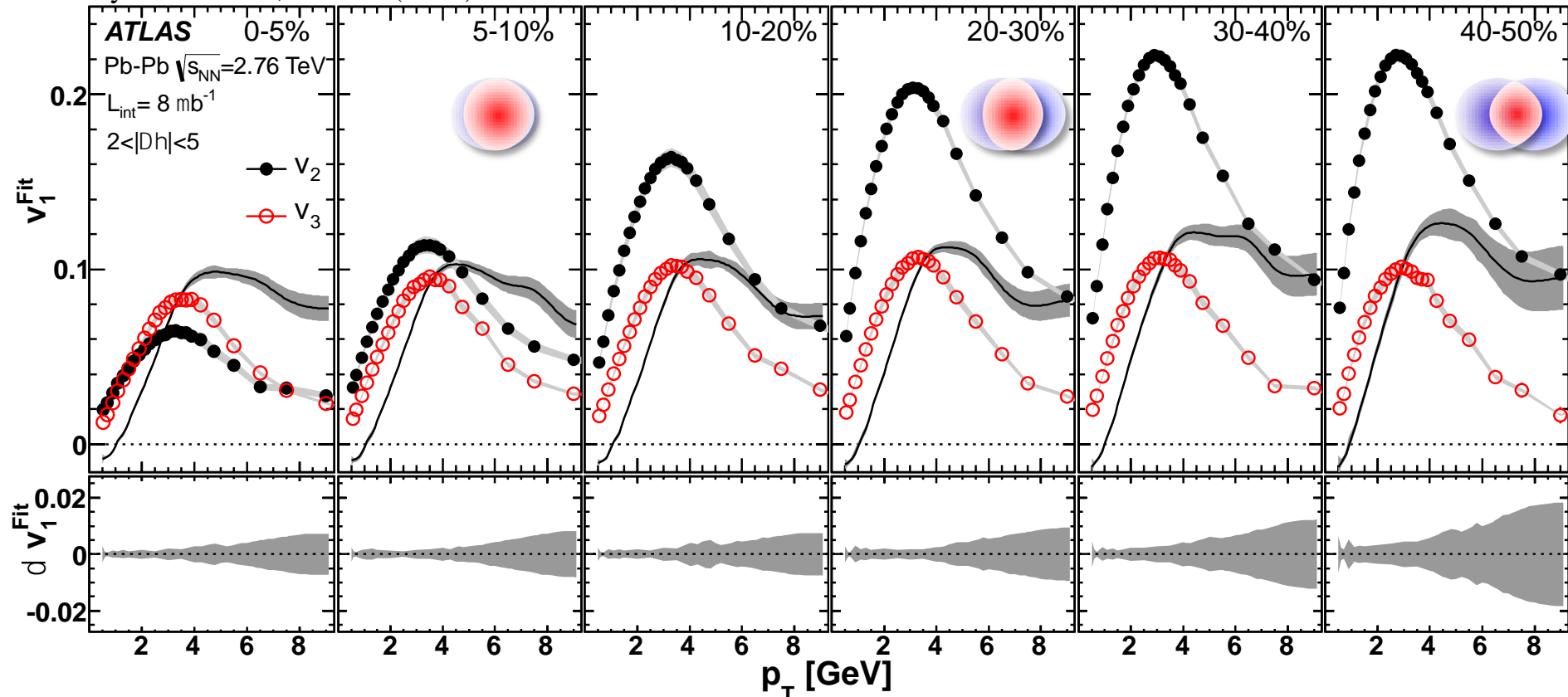
Red Points: $v_{1,1}$ data

Black line : Fit to functional form

Blue line: momentum conservation component

Extracted dipolar flow

Phys. Rev. C 86, 014907 (2012)



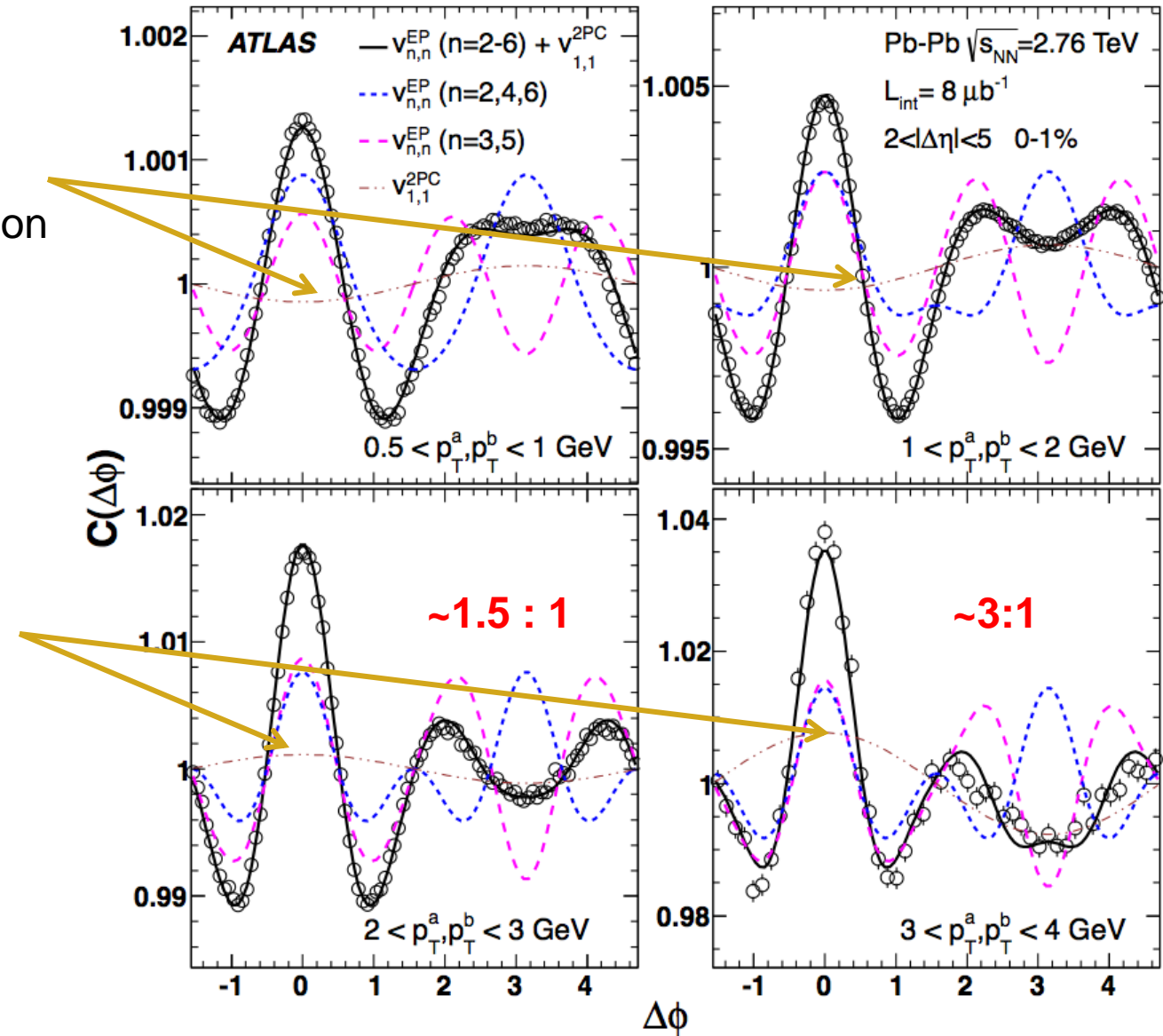
- Negative for $p_T < 1.0 \text{ GeV} \rightarrow$ expected from hydro calculations
 - Similar magnitudes as v_3 but much larger at high p_T
 - Large high $p_T v_1$ expected from L-dependence of energy loss
- 1203.3265

Importance of dipolar flow for 2PC (0-5%)

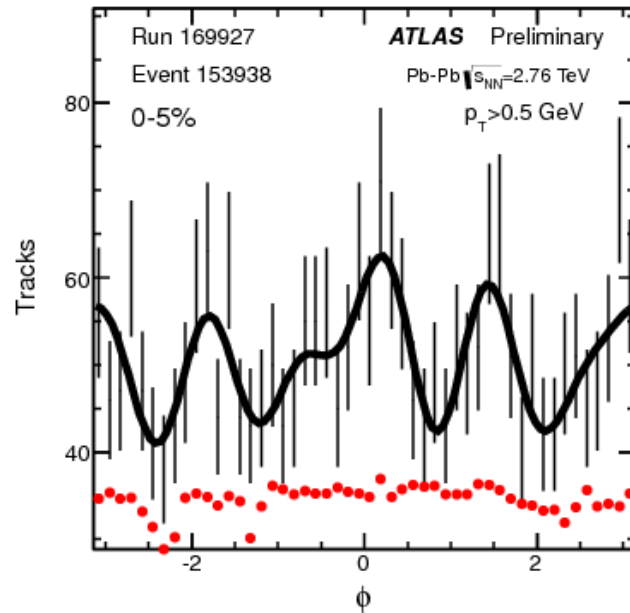
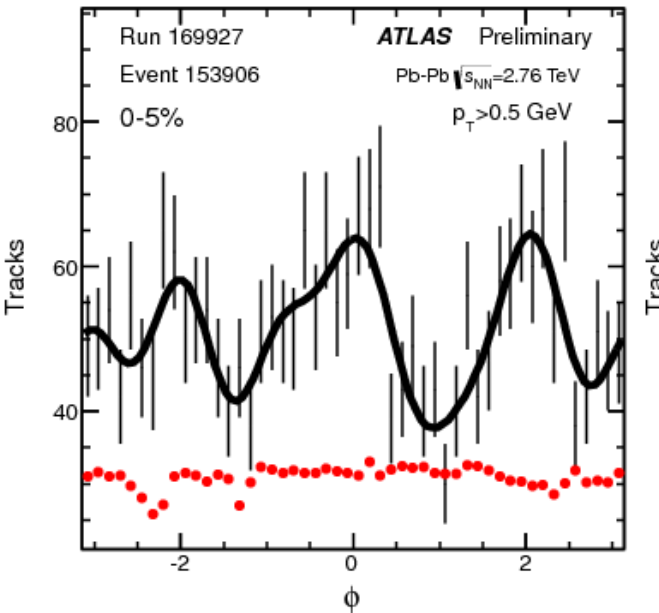
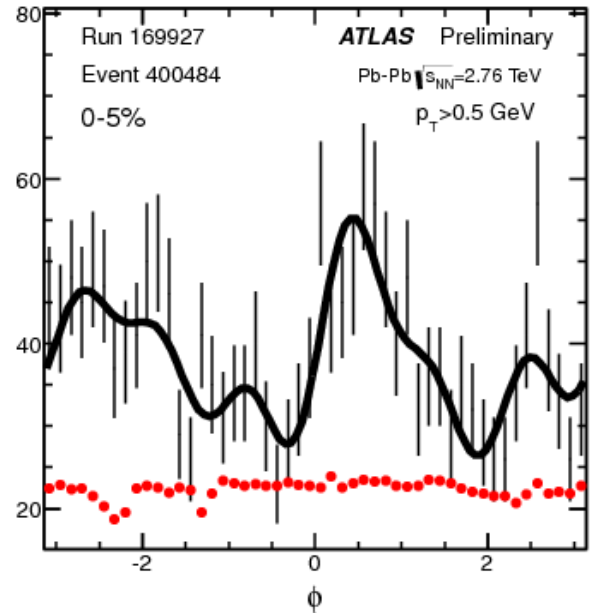
$v_{1,1}$ component shown by brown dashed lines

Most of $v_{1,1}$ is due to momentum conservation

Most of $v_{1,1}$ is due to dipolar flow



Flow observables



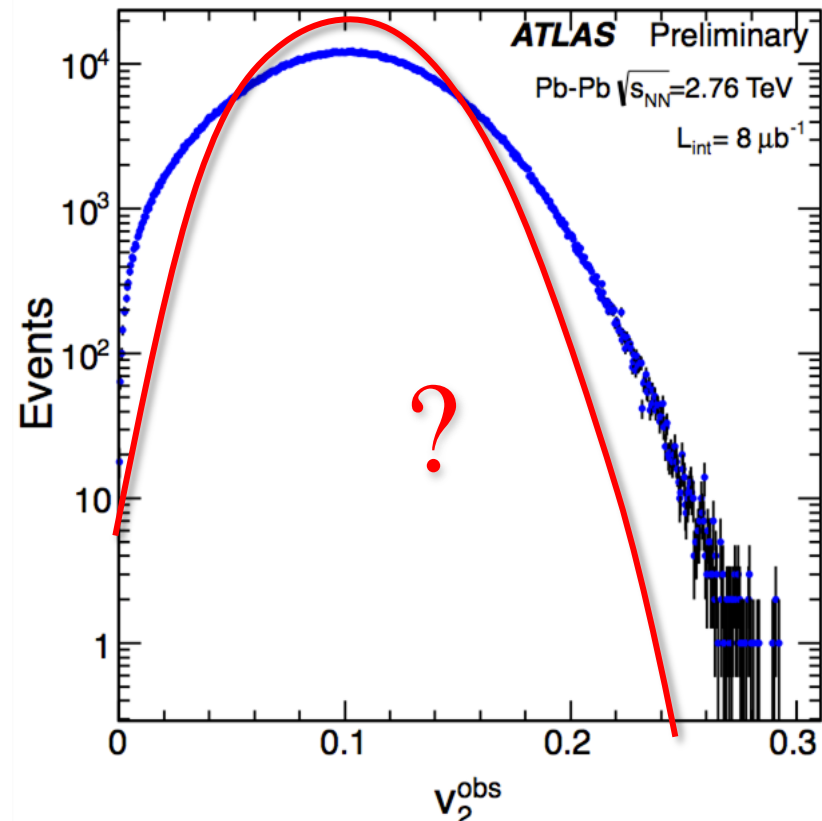
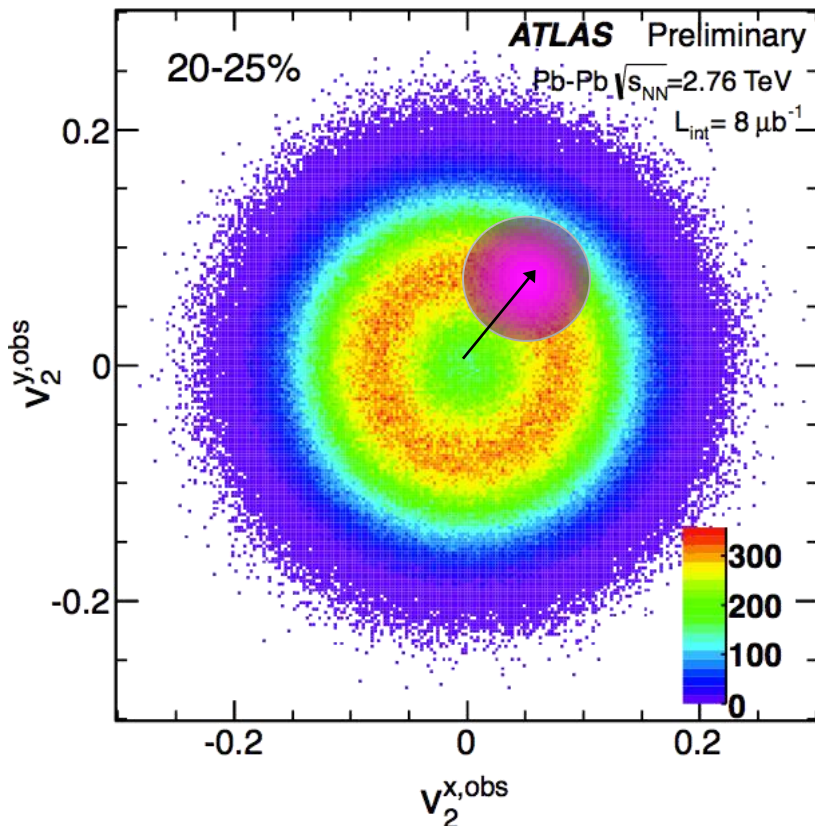
$$\frac{dN}{d\phi} \propto 1 + \sum_n 2v_n \cos n(\phi - \Phi_n)$$

- Mean values of $v_n(p_T, \eta, \text{cent})$. PhysRevC.86.014907
- Event by event v_n distributions. ATLAS-CONF-2012-114
- Correlations between flow phases Φ_n . ATLAS-CONF-2012-49

Flow vector and smearing

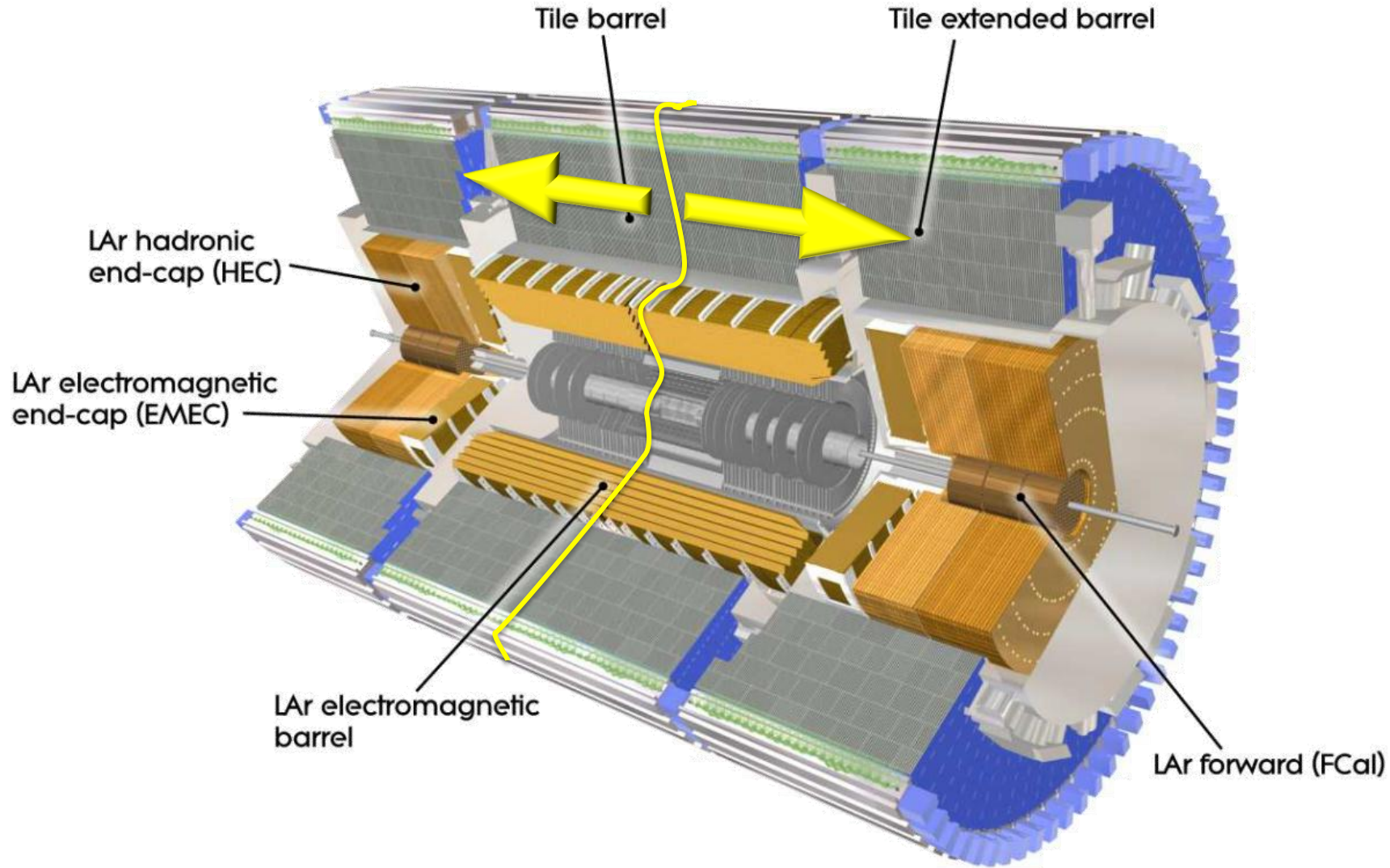
$$\frac{dN}{df} \propto 1 + 2\sum_n^{\infty} [v_{n,x}^{\text{obs}} \cos(nf) + v_{n,y}^{\text{obs}} \sin(nf)]$$

$$v_n^{\text{obs}} = (v_{n,x}^{\text{obs}}, v_{n,y}^{\text{obs}}) = v_n^{\text{true}} + p_n^{\text{smear}}$$



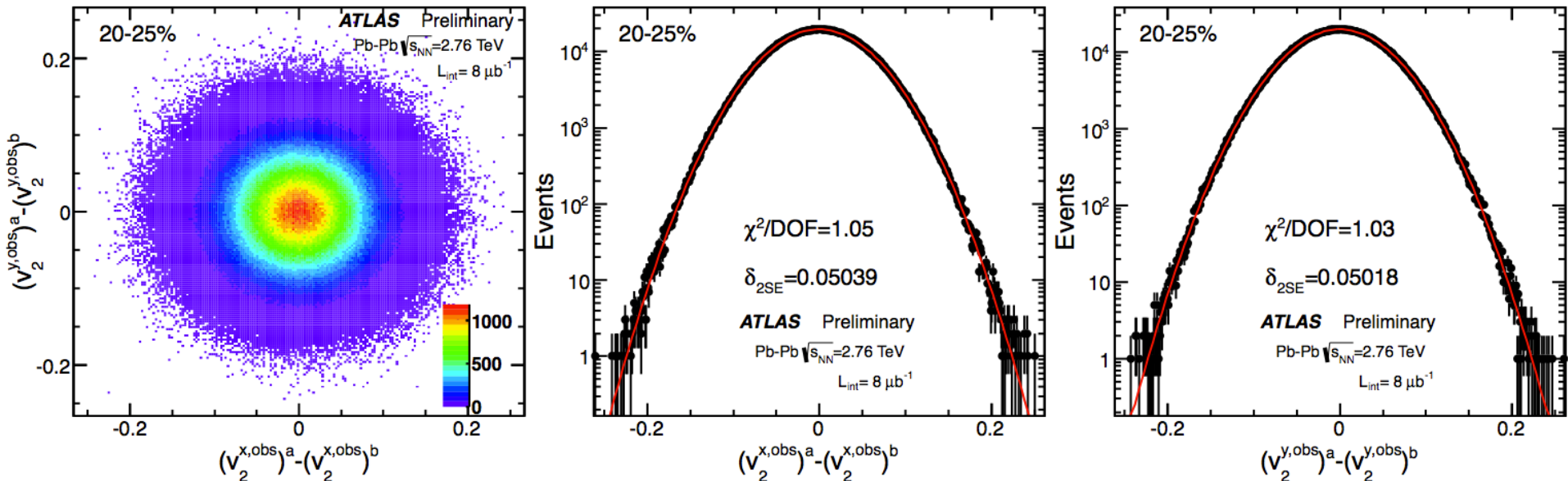
The key of unfolding is response function: $p(v_n^{\text{obs}} | v_n)$

Split the event into two



Sub-event “A” – Sub-event “C” = {
Signal: cancelled
Fluctuations: $\sqrt{2}$ larger

Obtaining the response function



2D response function is a 2D Gaussian

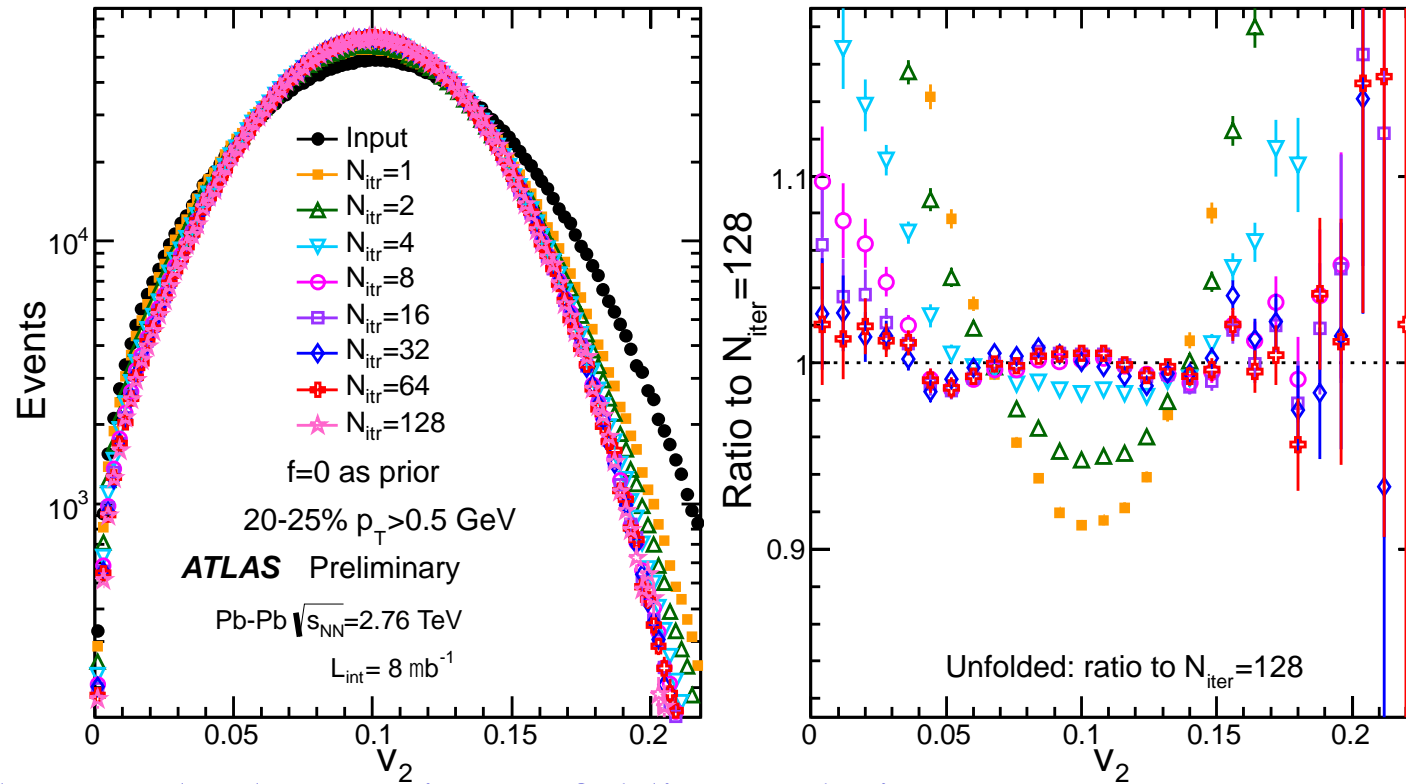
$$p(\vec{v}_n^{\text{obs}} | \vec{v}_n) \propto e^{-\frac{|\vec{v}_n^{\text{obs}} - \vec{v}_n|^2}{2\delta^2}} \quad \delta = \begin{cases} \delta_{2\text{SE}} / \sqrt{2} & \text{for half ID} \\ \delta_{2\text{SE}} / 2 & \text{for full ID} \end{cases}$$

1D response function obtained by integrating out azimuth angle

$$p(v_n^{\text{obs}} | v_n) \propto v_n^{\text{obs}} e^{-\frac{(v_n^{\text{obs}})^2 + v_n^2}{2\delta^2}} I_0\left(\frac{v_n^{\text{obs}} v_n}{\delta^2}\right)$$

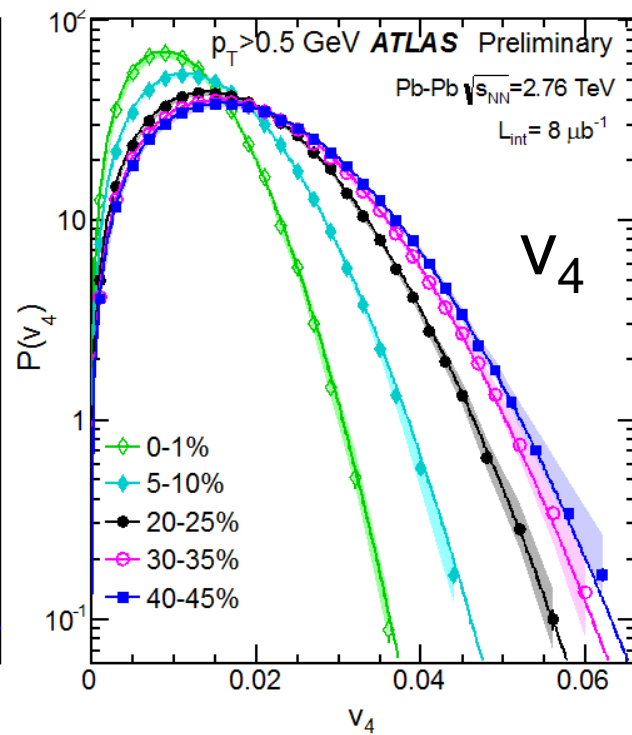
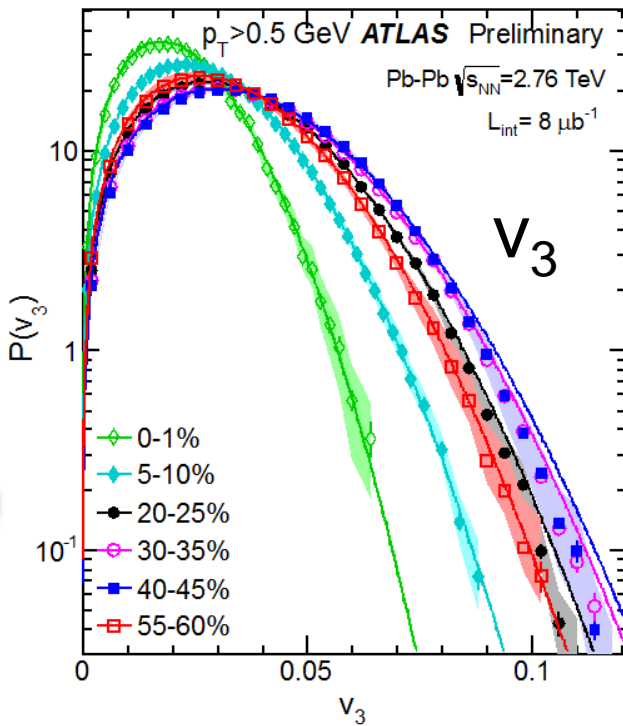
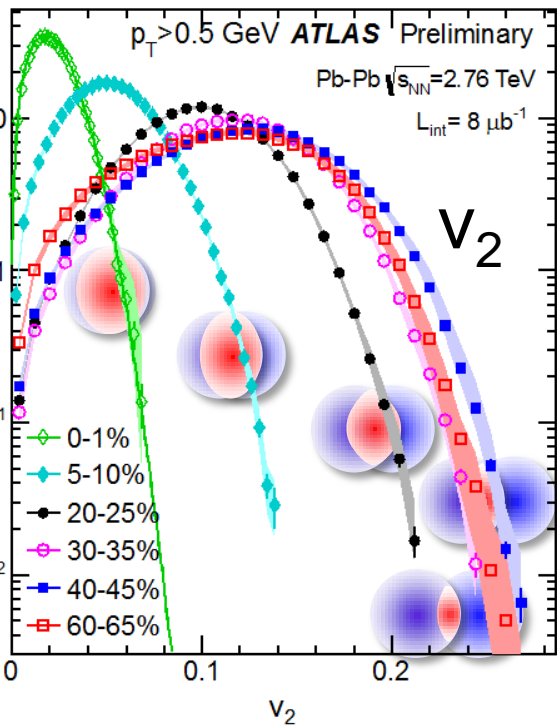
Data driven method

Unfolding performance: v_2 , 20-25%



- Use the standard Bayesian unfolding technique
 - Converges within a few % for $N_{\text{iter}}=8$, small improvements for larger N_{iter} .
 - Many cross checks show good consistency
 - Unfolding with different initial distributions
 - Unfolding using tracks in a smaller detector
 - Unfolding directly on the EbE two-particle correlation.
- Details in ATLAS-CONF-2012-114

Flow probability distributions

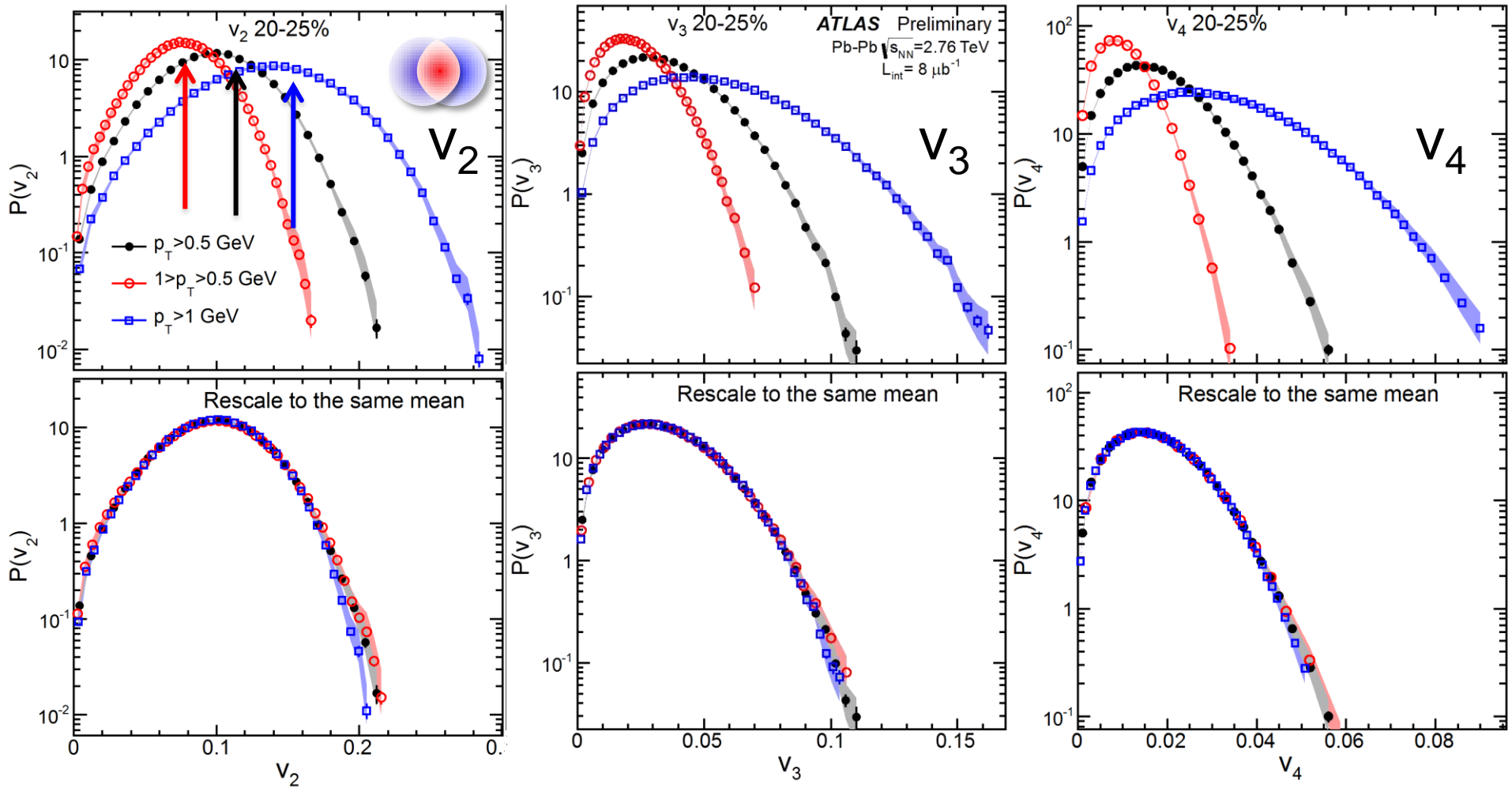


- v_n distributions corrected for detector effect and finite multiplicity
- v_2 in central, and v_3 v_4 in all centrality are described by a radial

Gaussian function: $P(v_n) = \frac{v_n}{\sigma^2} e^{-\frac{v_n^2}{2\sigma^2}}$ → driven by Gaussian fluctuation

$$\frac{\sigma_{v_n}}{\langle v_n \rangle} = \sqrt{\frac{4}{\pi} - 1} = 0.523 \quad \sqrt{\langle v_n^2 \rangle} = \frac{2}{\sqrt{\pi}} \langle v_n \rangle = 1.13 \langle v_n \rangle$$

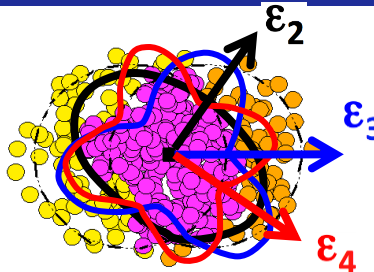
p_T -scaling of the probability distribution



All p_T bins have similar shape, hold for all n .

Hydrodynamic response \sim independent of p_T .

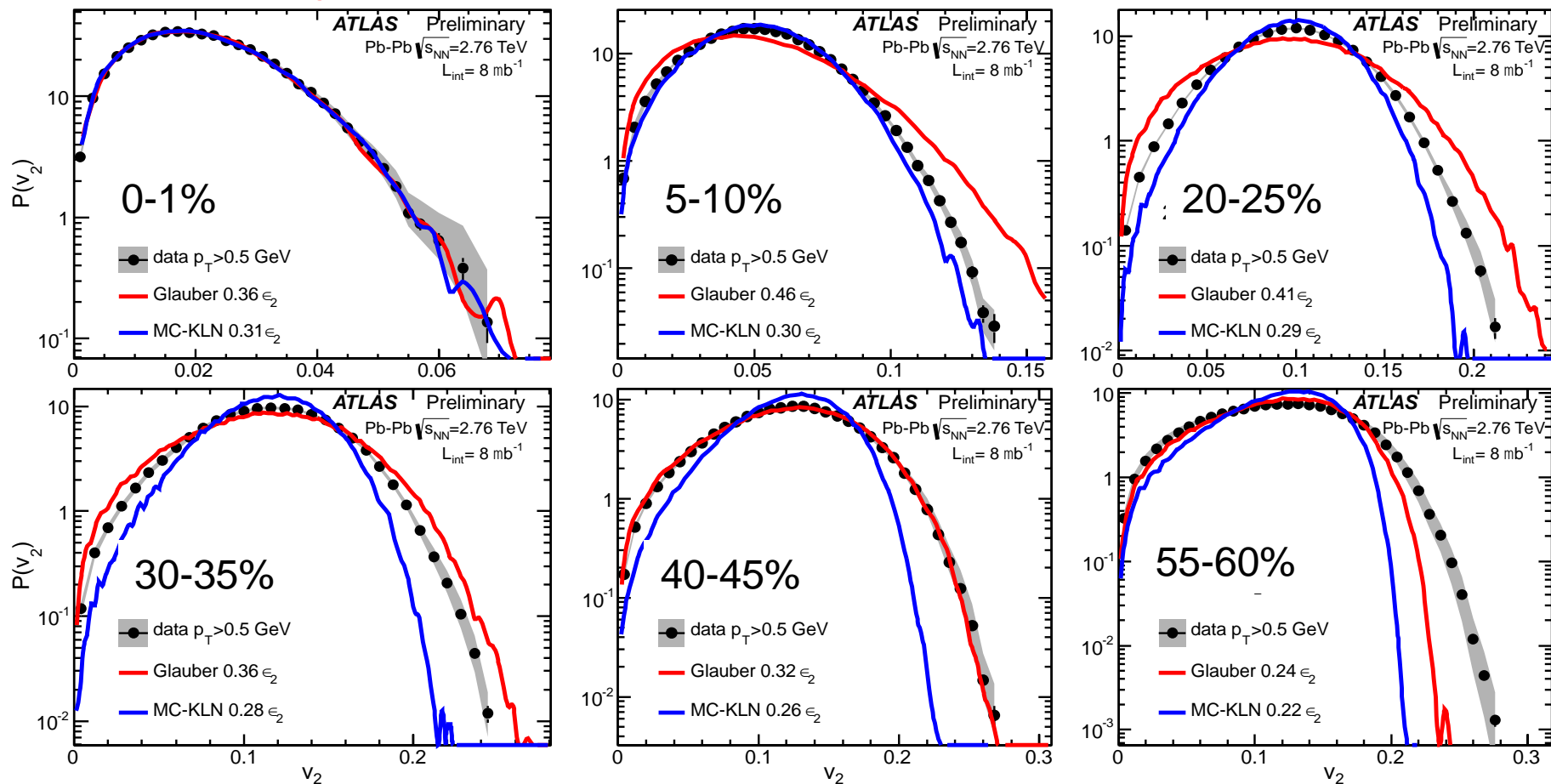
Measuring the hydrodynamic response



$$v_n \propto \epsilon_n = \frac{\sqrt{\langle r^n \cos n\phi \rangle^2 + \langle r^n \sin n\phi \rangle^2}}{\langle r^n \rangle}$$

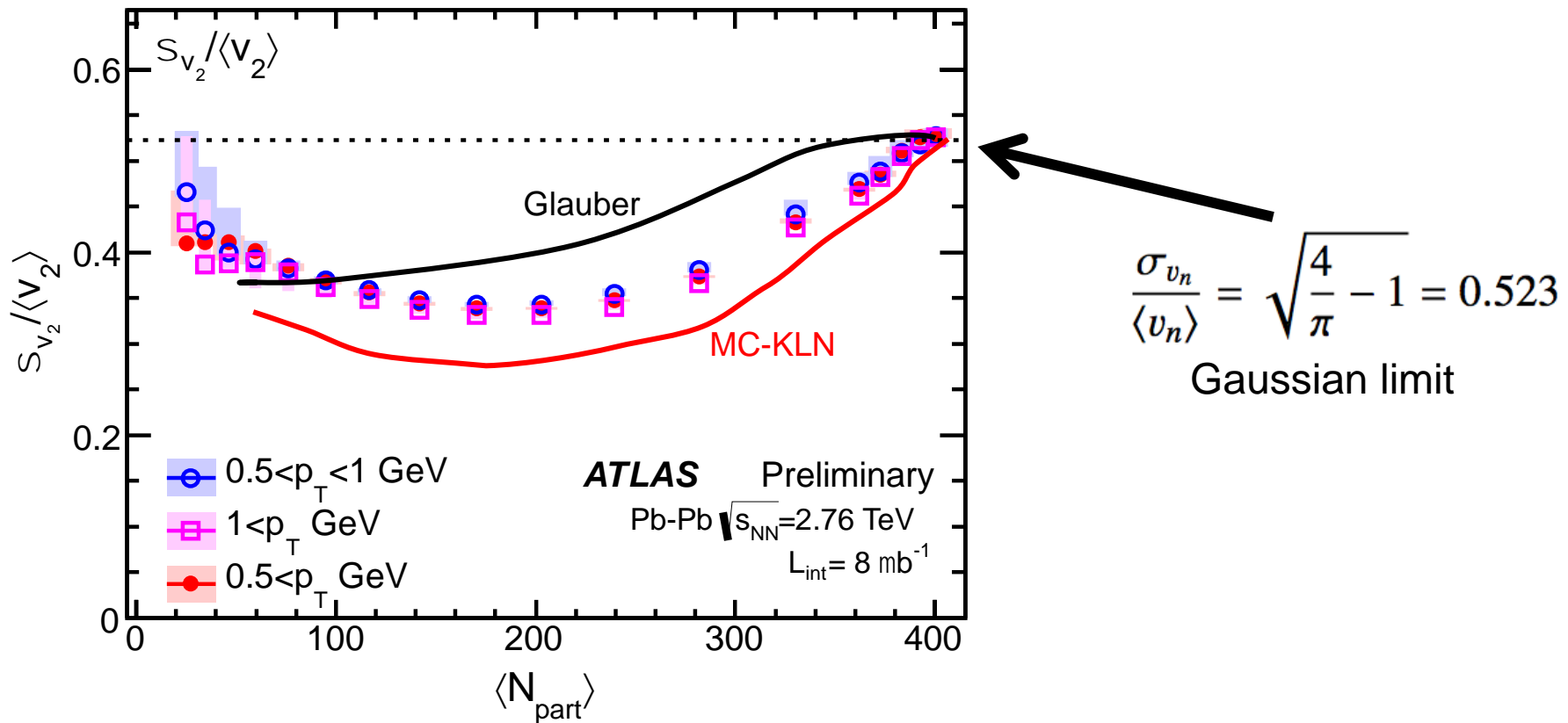
Glauber and CGC mckln

Rescale ϵ_n distribution to the mean of data



Both models fail describing $p(v_2)$ across the full centrality range

Relative fluctuations: width/mean for v_2



- Direct precision measurement of the relative fluctuations
 - Consistent with but more precise than those obtained indirectly from cumulant method

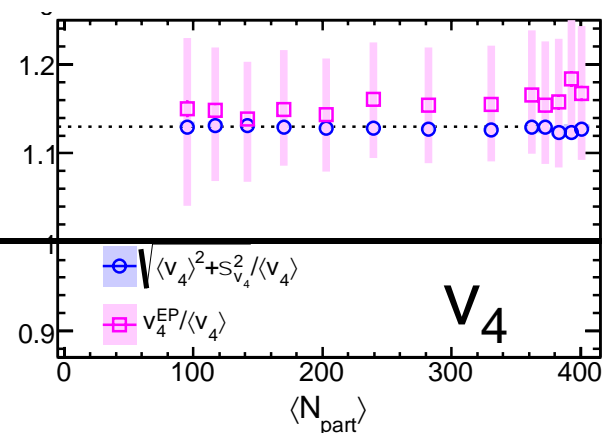
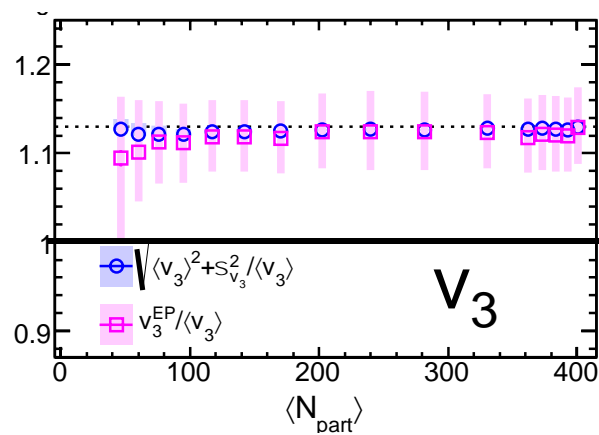
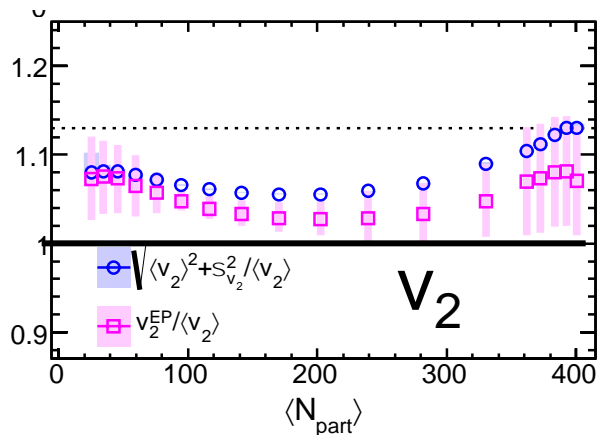
$$\frac{\sigma_2}{\langle v_2 \rangle} \approx \sqrt{\frac{v_2\{2\}^2 - v_2\{4\}^2}{v_2\{2\}^2 + v_2\{4\}^2}}$$

What does event plane v_n measure?

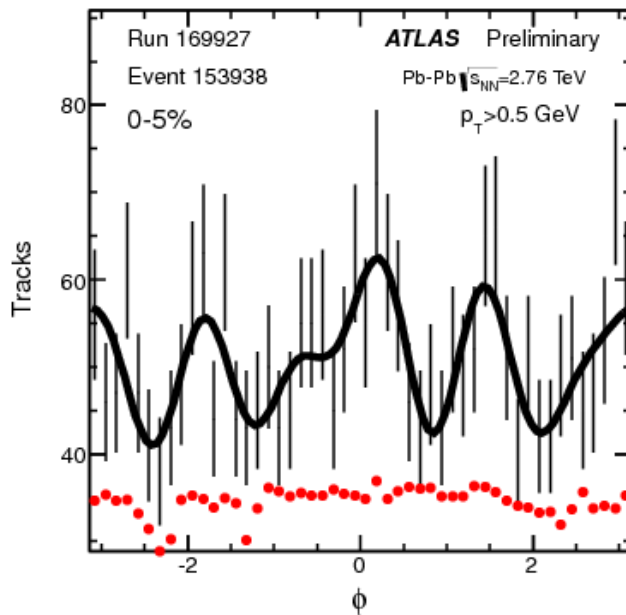
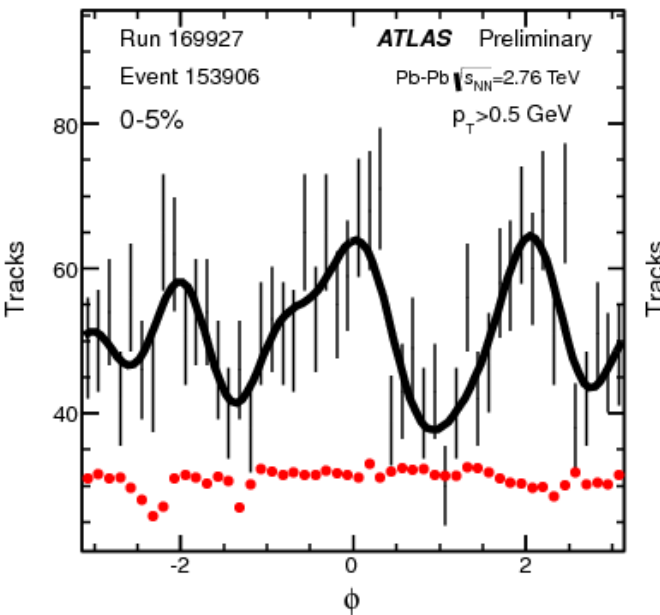
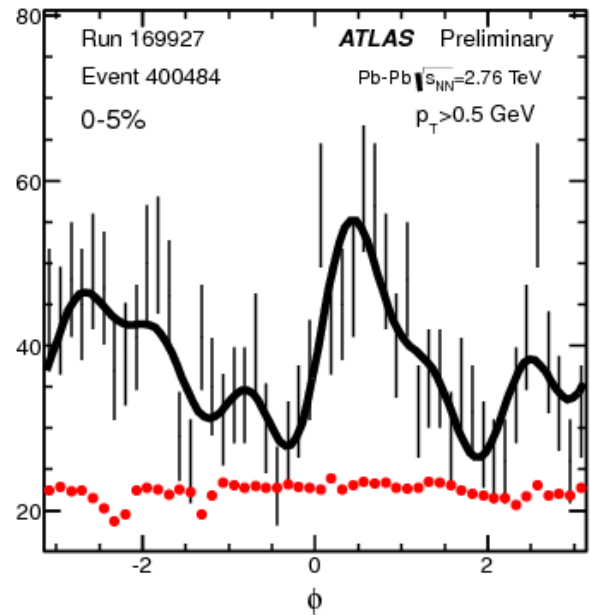
- Expectations: $\langle v_n \rangle \leq v_n^{\text{EP}} \leq \sqrt{\langle v_n^2 \rangle} = \sqrt{\langle v_n \rangle^2 + \sigma_{v_n}^2}$. **Verified!!**

○ $\sqrt{v_n^2 / \langle v_n \rangle}$
□ $v_n^{\text{EP}} / \langle v_n \rangle$

ATLAS EP $v_n \approx \sqrt{v_n^2}$ within few %



Flow observables



$$\frac{dN}{d\phi} \propto 1 + \sum_n 2v_n \cos n(\phi - \Phi_n)$$

- Mean values of $v_n(p_T, \eta, \text{cent})$. PhysRevC.86.014907
- Event by event v_n distributions. ATLAS-CONF-2012-114
- Correlations between flow phases Φ_n . ATLAS-CONF-2012-49

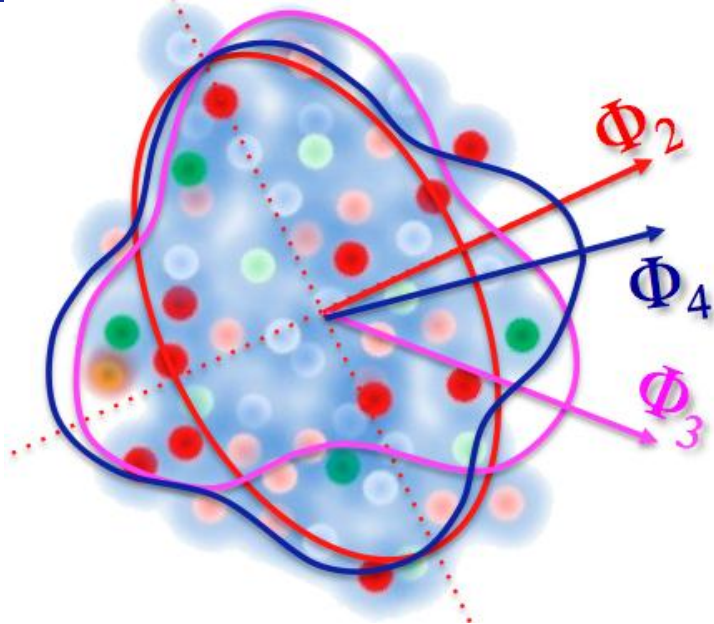
Correlation between phases of harmonic flow

- Correlation can exist in the initial geometry and also generated during hydro evolution
- The correlation can be quantify via a set of simple correlators

arXiv:1205.3585
arXiv:1203.5095

$$\frac{dN_{events}}{d(k(\mathcal{F}_n - \mathcal{F}_m))} = 1 + 2 \sum_{j=1}^{\infty} V_{n,m}^j \cos(jk(\mathcal{F}_n - \mathcal{F}_m))$$

$$V_{n,m}^j = \langle \cos(jk(\mathcal{F}_n - \mathcal{F}_m)) \rangle$$



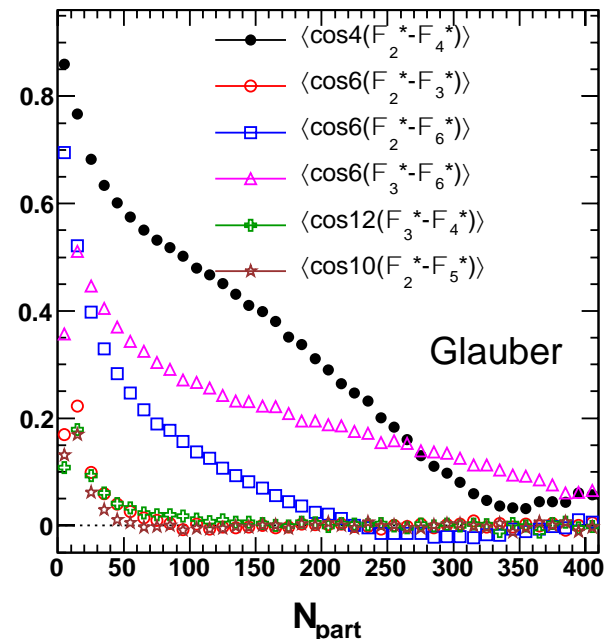
- Measured quantity need to be corrected by resolution

$$\langle \cos(jk(\mathcal{F}_n - \mathcal{F}_m)) \rangle = \frac{\langle \cos(jk(\mathcal{Y}_n - \mathcal{Y}_m)) \rangle}{\text{Res}(jk \mathcal{Y}_n) \text{Res}(jk \mathcal{Y}_m)}$$

$\mathcal{F}_n = True$, $\mathcal{Y}_n = Measured$

- This can be generalized into multi-plane correlations

$$\langle \cos(c_1 \mathcal{F}_1 + 2c_2 \mathcal{F}_2 + \dots + c_l \mathcal{F}_l) \rangle \quad c_1 + 2c_2 + \dots + c_l = 0$$



A list of measured correlators

- List of two-plane correlators

$$\begin{aligned}
 & \langle \cos 4(\Phi_2 - \Phi_4) \rangle \\
 & \langle \cos 8(\Phi_2 - \Phi_4) \rangle \\
 & \langle \cos 12(\Phi_2 - \Phi_4) \rangle \\
 & \langle \cos 6(\Phi_2 - \Phi_3) \rangle \\
 & \langle \cos 6(\Phi_2 - \Phi_6) \rangle \\
 & \langle \cos 6(\Phi_3 - \Phi_6) \rangle \\
 & \langle \cos 12(\Phi_3 - \Phi_4) \rangle \\
 & \langle \cos 10(\Phi_2 - \Phi_5) \rangle
 \end{aligned}$$

- List of three-plane correlators

“2-3-5”

$$\begin{aligned}
 & \langle \cos(2\Phi_2 + 3\Phi_3 - 5\Phi_5) \rangle \\
 & \langle \cos(-8\Phi_2 + 3\Phi_3 + 5\Phi_5) \rangle
 \end{aligned}$$

“2-4-6”

$$\begin{aligned}
 & \langle \cos(2\Phi_2 + 4\Phi_4 - 6\Phi_6) \rangle \\
 & \langle \cos(-10\Phi_2 + 4\Phi_4 + 6\Phi_6) \rangle
 \end{aligned}$$

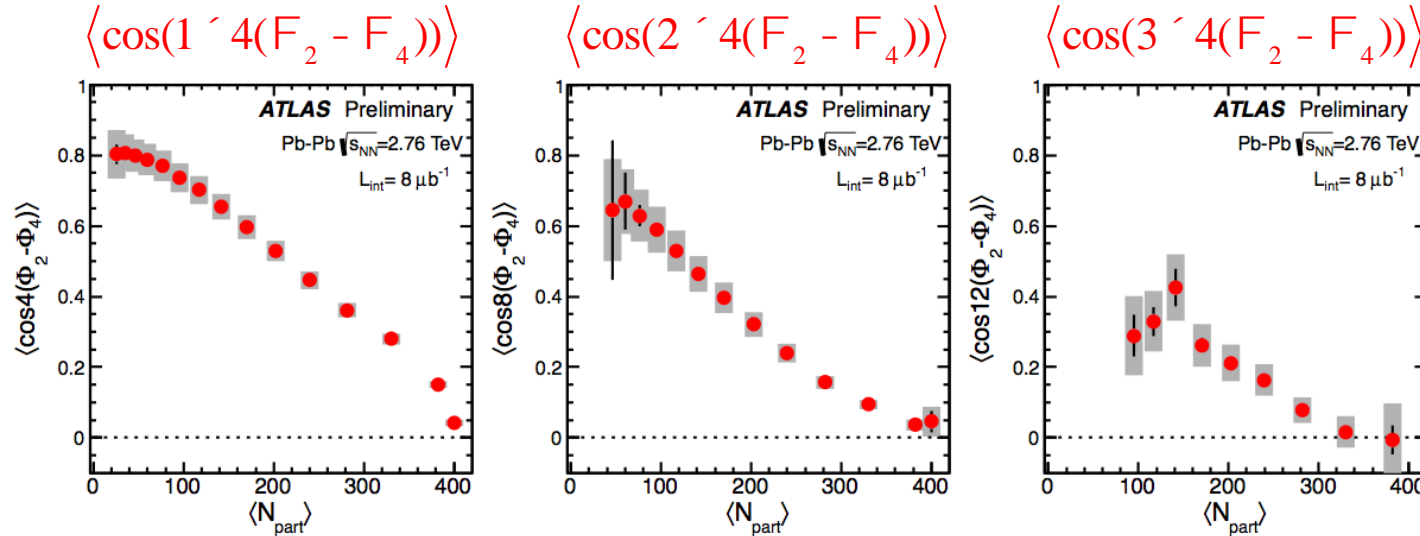
“2-3-4”

$$\begin{aligned}
 & \langle \cos(2\Phi_2 - 6\Phi_3 + 4\Phi_4) \rangle \\
 & \langle \cos(-10\Phi_2 + 6\Phi_3 + 4\Phi_4) \rangle
 \end{aligned}$$

$$\begin{aligned}
 2\Phi_2 + 4\Phi_4 - 6\Phi_6 &= 4(\Phi_4 - \Phi_2) - 6(\Phi_6 - \Phi_2) \\
 -10\Phi_2 + 4\Phi_4 + 6\Phi_6 &= 4(\Phi_4 - \Phi_2) + 6(\Phi_6 - \Phi_2)
 \end{aligned}$$

Reflects correlation of two Φ_n relative to the third

Two-plane correlations



$$\nu_6 e^{-i 6 Y_6} = \text{geometry} + \nu_2 \nu_2 \nu_2 e^{-i 6 Y_2} + \nu_3 \nu_3 e^{-i 6 Y_3} + \dots$$

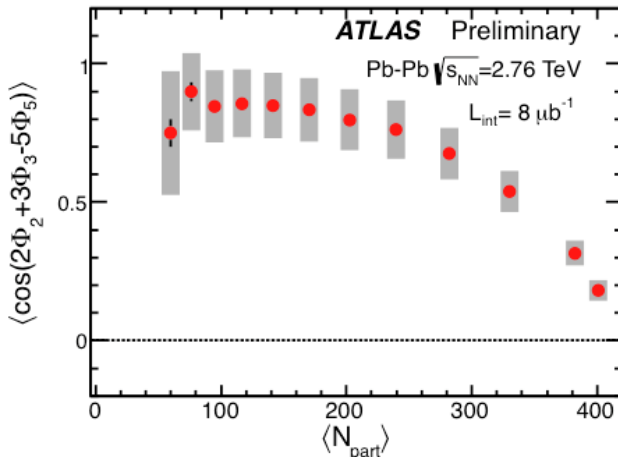
Teany & Yan

Rich centrality dependence patterns

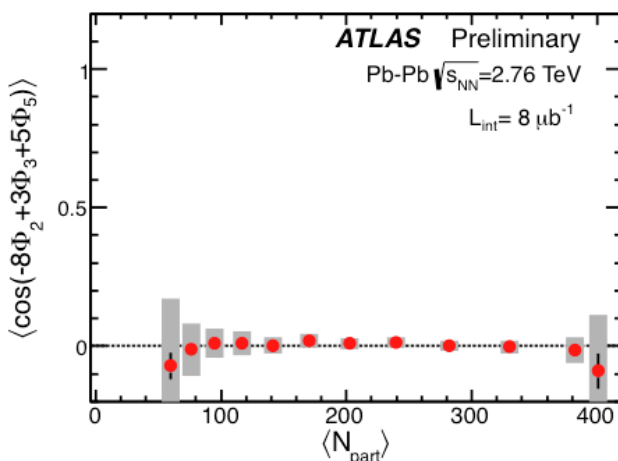
Three-plane correlations

“2-3-5” correlation

$$\langle \cos(2\Phi_2 + 3\Phi_3 - 5\Phi_5) \rangle$$

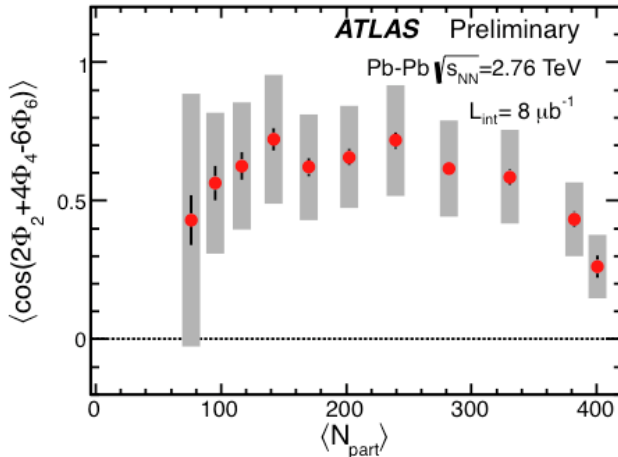


$$\langle \cos(-8\Phi_2 + 3\Phi_3 + 5\Phi_5) \rangle$$

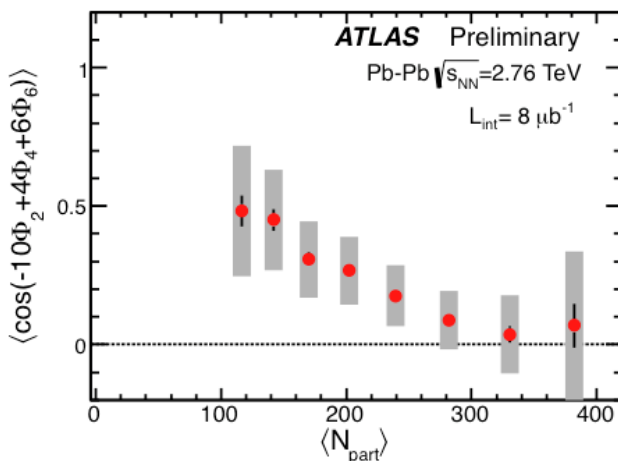


“2-4-6” correlation

$$\langle \cos(2\Phi_2 + 4\Phi_4 - 6\Phi_6) \rangle$$

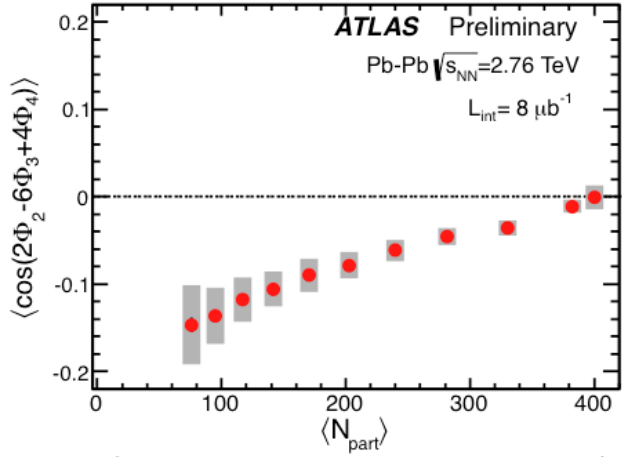


$$\langle \cos(-10\Phi_2 + 4\Phi_4 + 6\Phi_6) \rangle$$

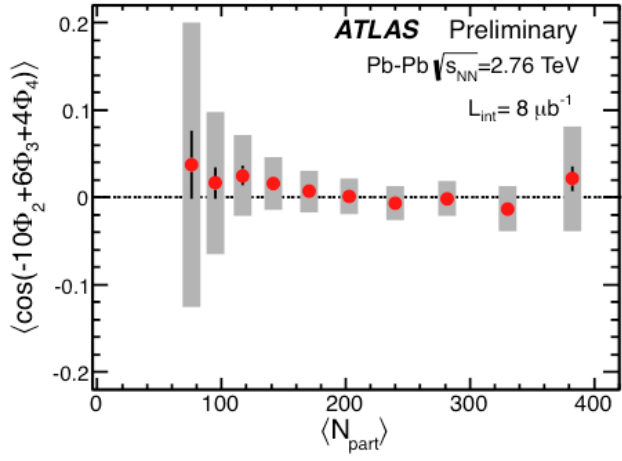


“2-3-4” correlation

$$\langle \cos(2\Phi_2 - 6\Phi_3 + 4\Phi_4) \rangle$$



$$\langle \cos(-10\Phi_2 + 6\Phi_3 + 4\Phi_4) \rangle$$



Rich centrality dependence patterns

Compare with EbE hydro calculation: 2-plane

Initial geometry
+ hydrodynamic

ATLAS data

MC-Glb., $\eta/s = 0.08$

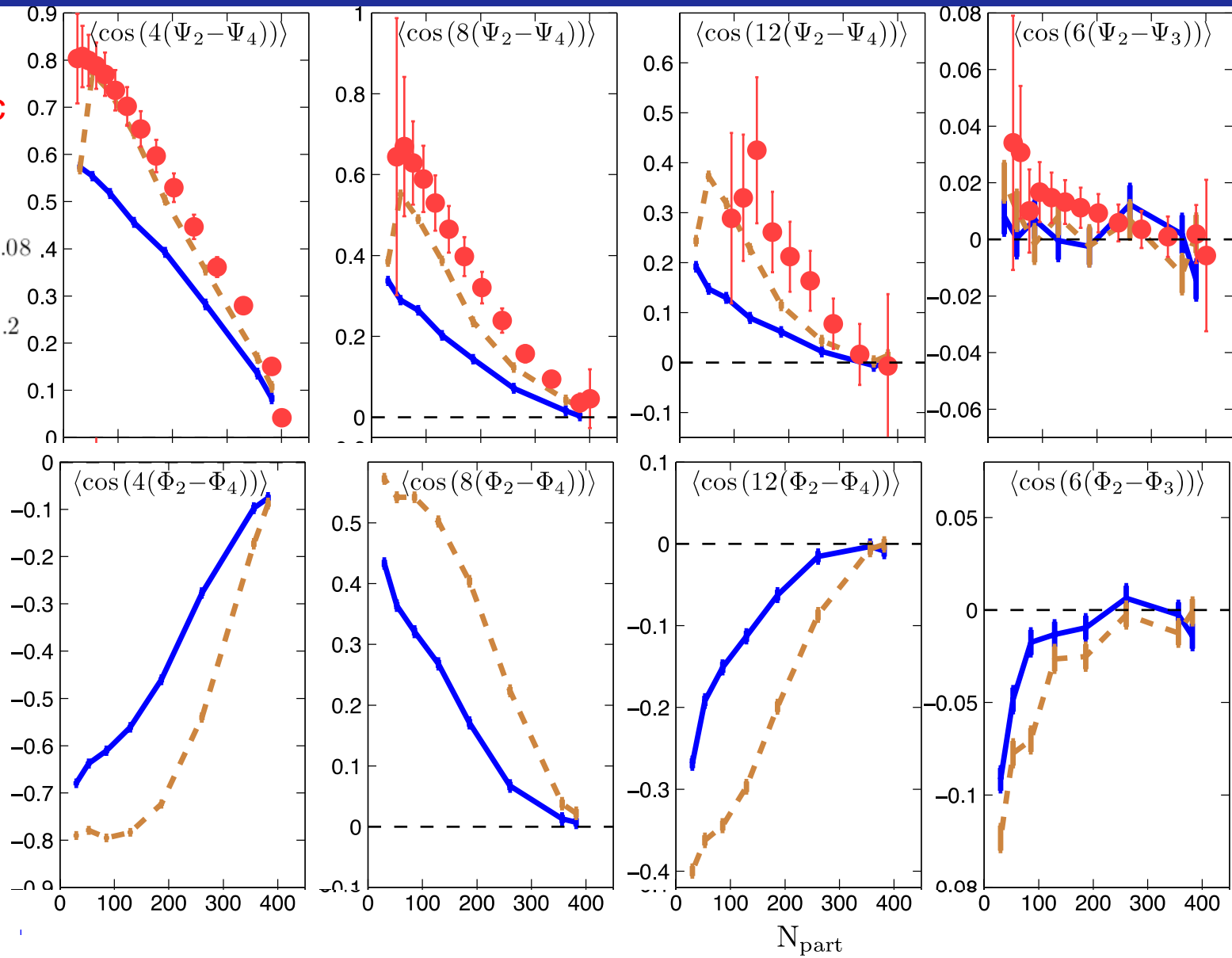
MC-KLN, $\eta/s = 0.2$

Zhe & Heinz

geometry only

MC-Glb.

MC-KLN,



EbE hydro qualitatively reproduce features in the data

Compare with EbE hydro calculation: 3-plane

Initial geometry
+ hydrodynamic

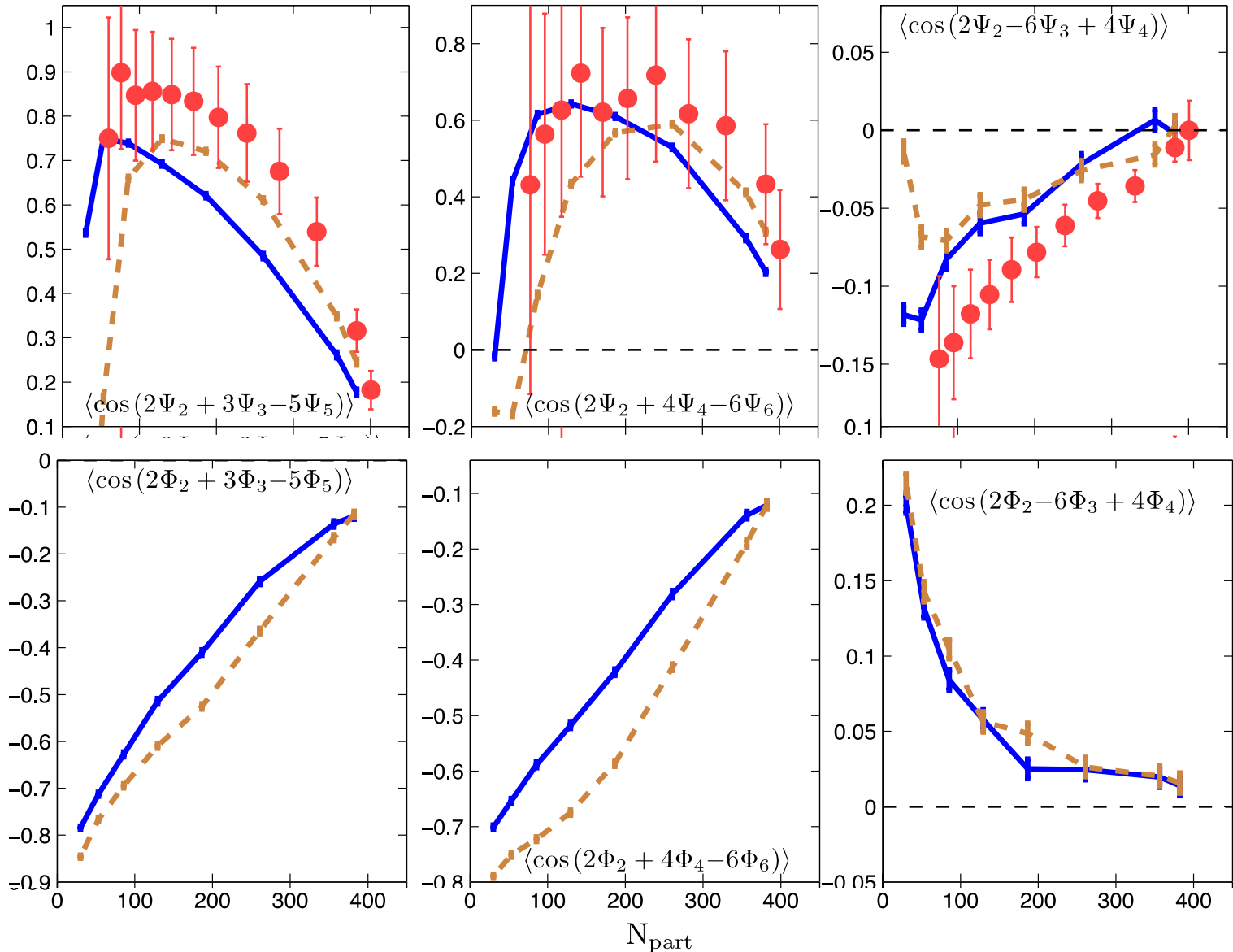
ATLAS data

MC-Glb., $\eta/s = 0.08$
MC-KLN, $\eta/s = 0.2$

Zhe & Heinz

geometry only

MC-Glb.
MC-KLN

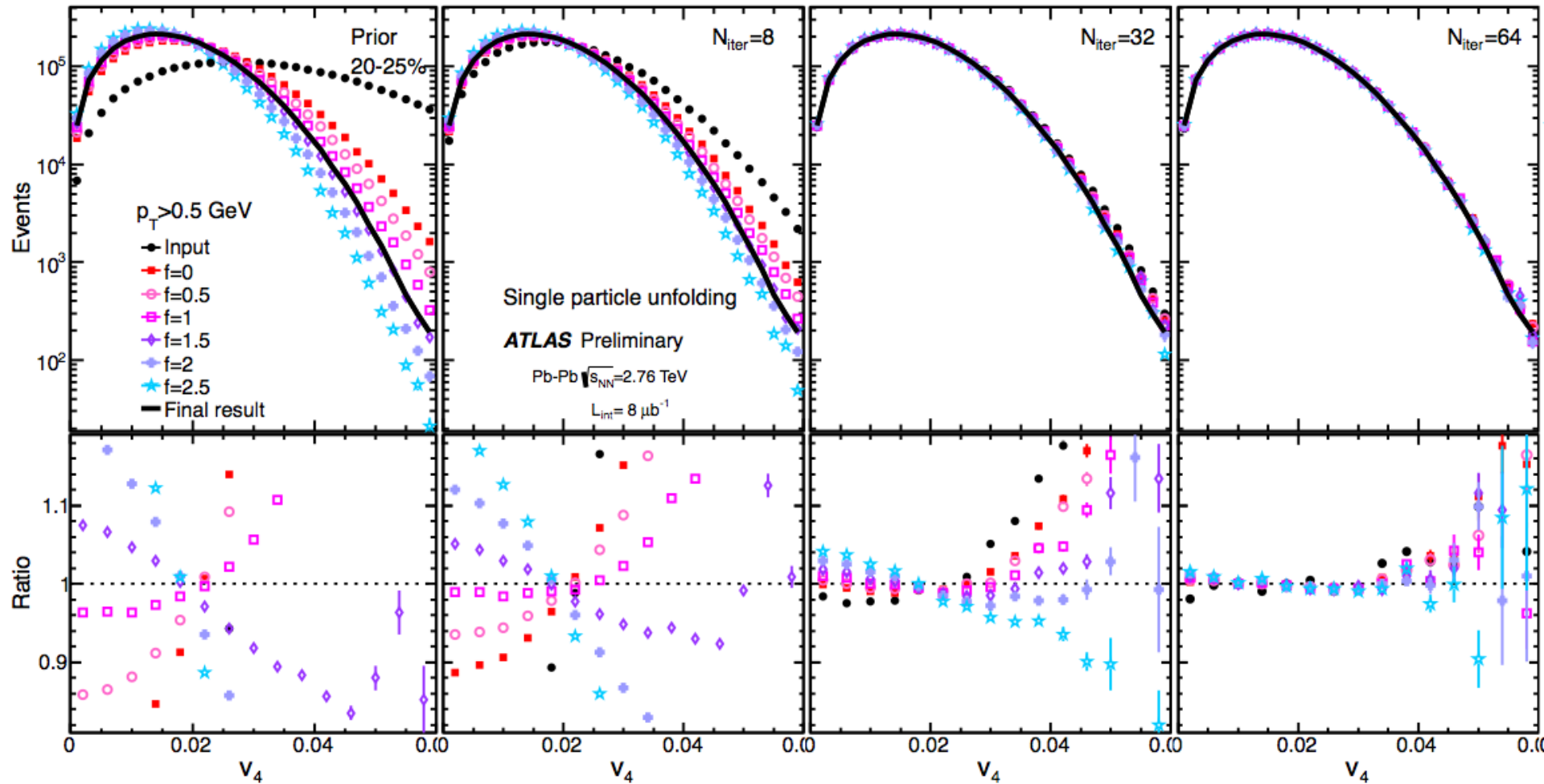


EbE hydro qualitatively reproduce features in the data

Summary

- Detailed differential measurement of $v_n(p_T, \eta, \text{centrality})$ for $n=1-6$
 - Factorization of $v_{n,n}$ to v_n works well for $n=2-6$, but breaks for $n=1$
 - dipolar flow v_1 extracted from $v_{1,1}$ via a two component fit.
 - v_1 magnitude comparable to v_3 , indicating significant dipole deformation in the initial state. High $p_T v_1$ may reflect L dependence of energy loss
- Event-by-event probability distribution of v_2-v_4
 - Consistent with Gaussian fluctuation for v_2 in central and v_3, v_4 in all centralities
 - The shape has no p_T dependence → hydro response independent of p_T
 - Glauber & MC-KLN model fails to describe the shape for all centralities.
 - Event plane $v_n \sim \text{RMS } v_n$ for $n=3-4$, but is in between RMS and mean for $n=2$
- Many correlations between two and three event planes
 - Some correlations qualitatively similar to Glauber model, many are not
 - Provides new constraints for initial geometry as well as hydro models

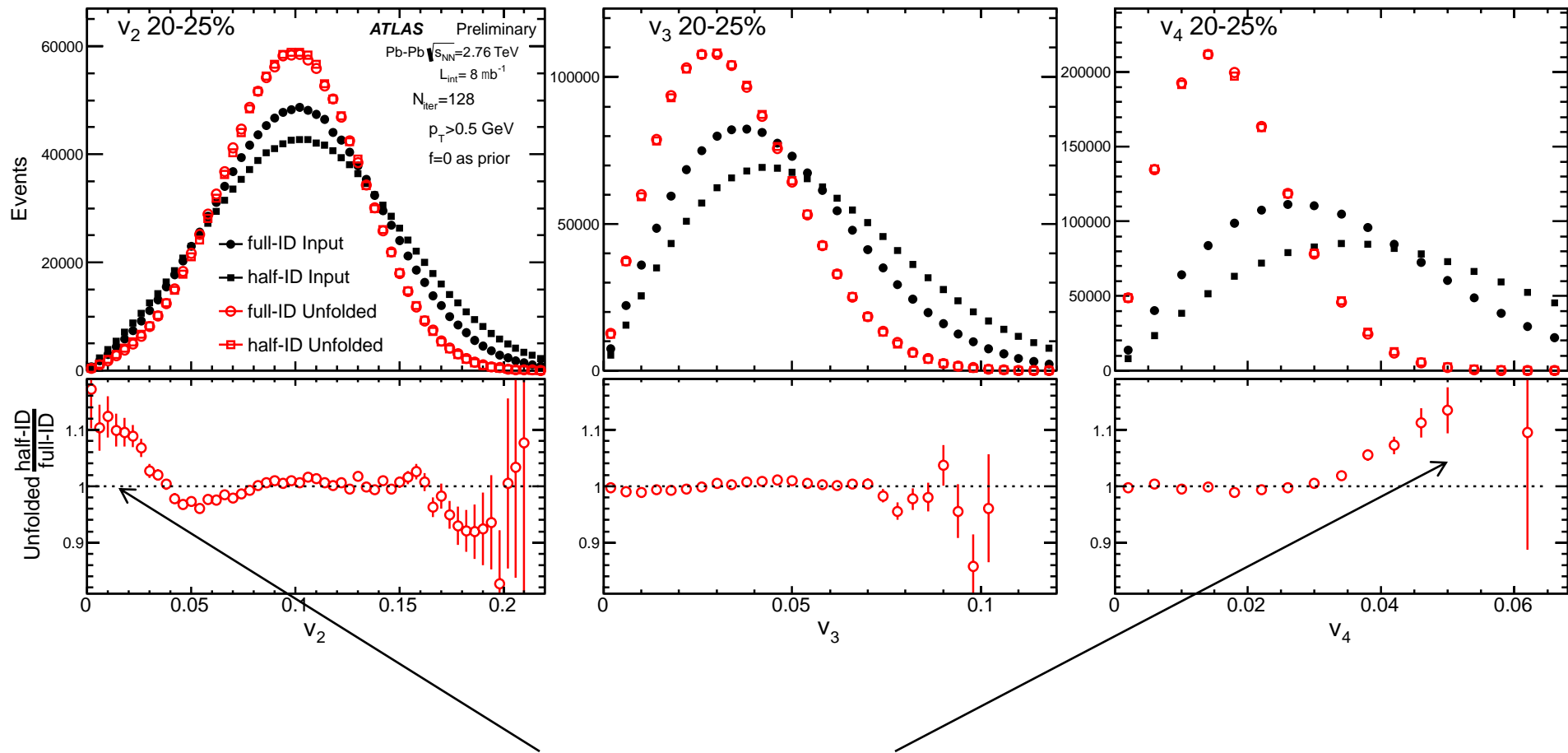
Dependence on prior: v_4 20-25%



- Despite different initial distribution, all converged for $N_{\text{iter}}=64$
- Wide prior converges from above, narrow prior converges from below! Provide constrains on the residual non-convergence

Compare to unfolding for half-ID: 20-25%

- Agrees within a few % in most cases, but can be larger in the tails, which mainly reflects the non-convergence of half-ID (since width of its response function is $\sqrt{2}$ wider)



Residual non-convergence of half-ID

Compare single & 2PC unfolding with η gaps

36

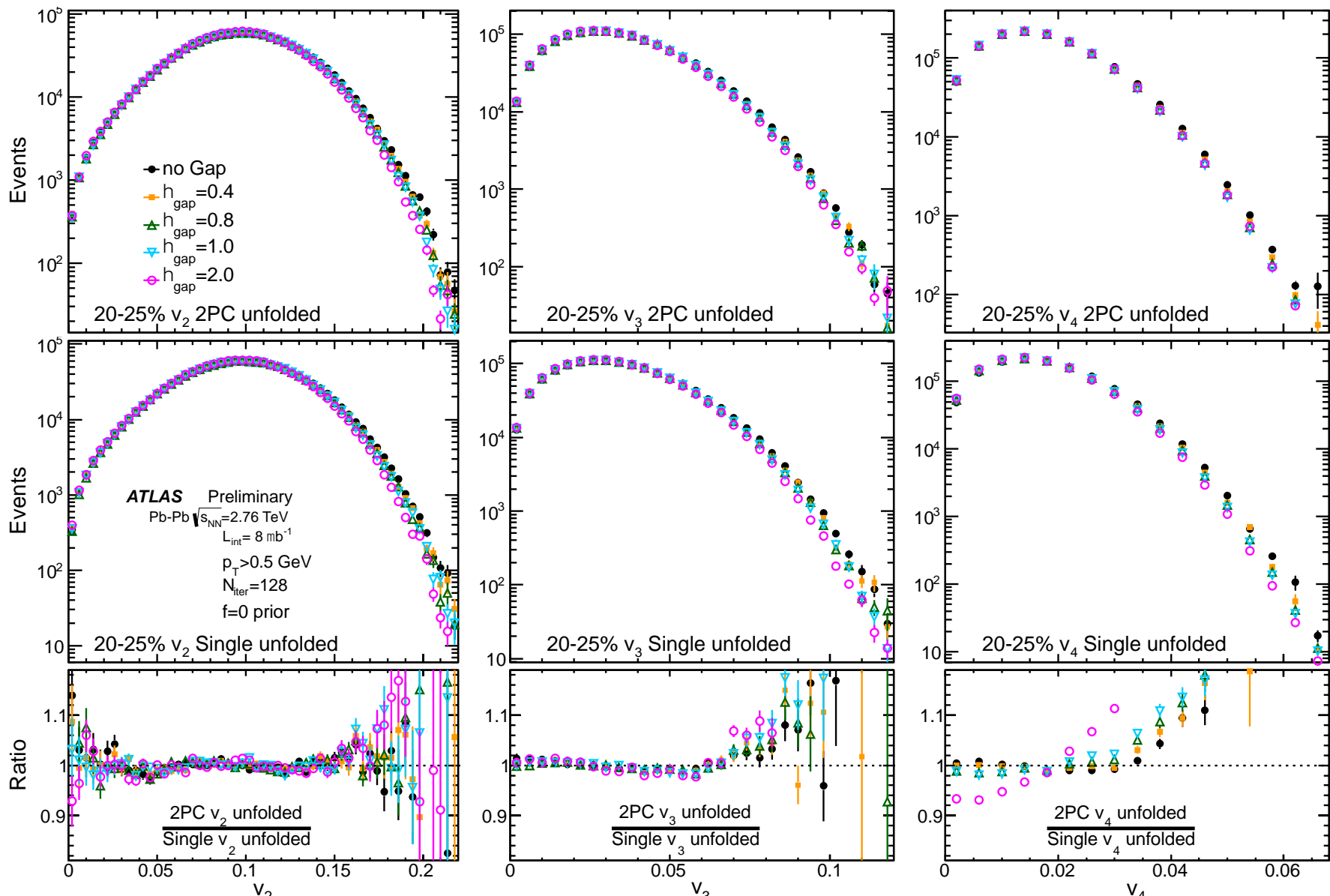
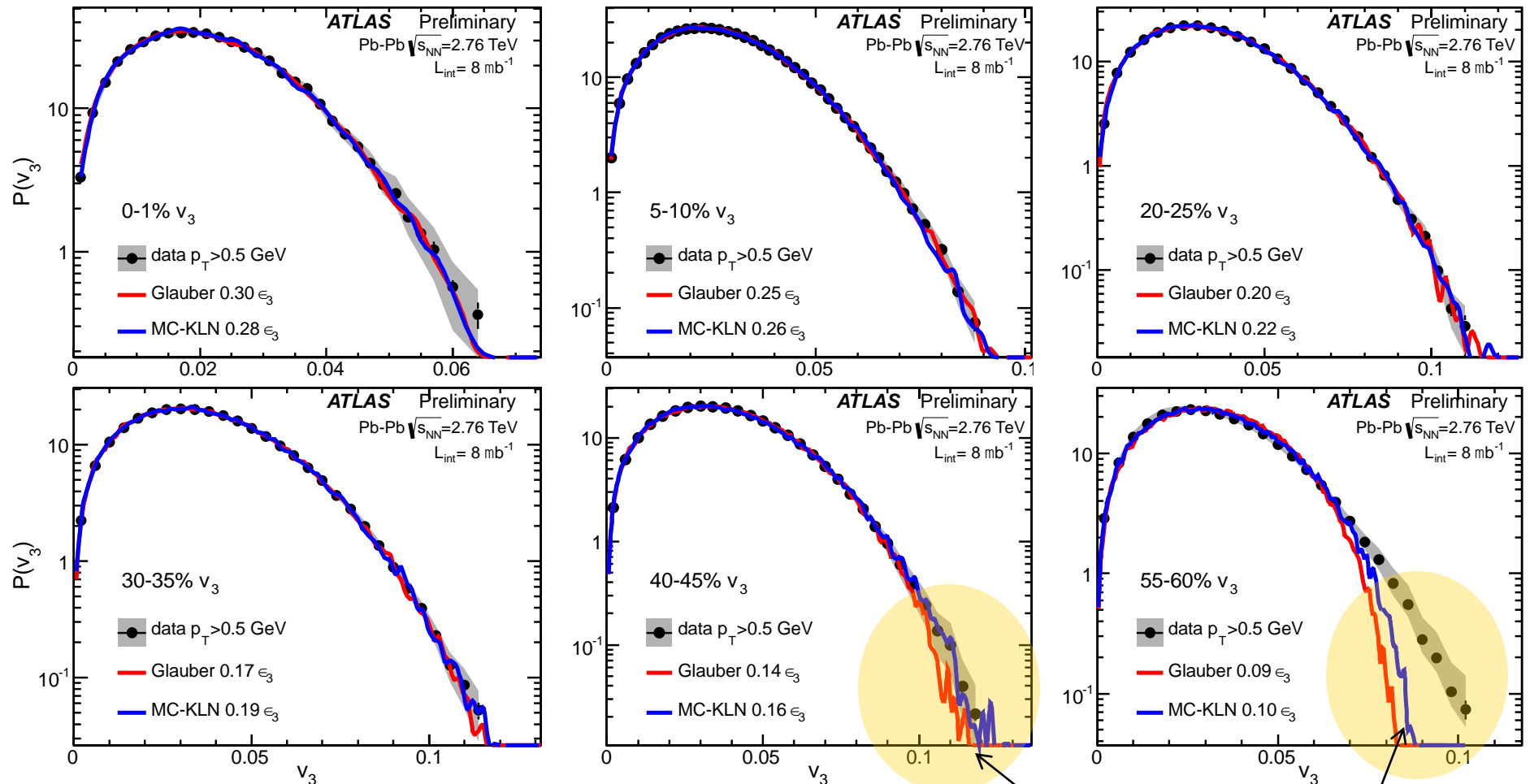


Figure 21: The unfolded distributions from 2PC method (top row), single particle method (middle row) and the ratios between the two (bottom row) for different values of η_{gap} in the 20-25% centrality interval and for $n = 2$ (left column), $n = 3$ (middle column) and $n = 4$ (right column).

How about v_3 ?



- Good agreement except in peripheral collisions, but this could be trivial, since all Gaussian functions have same reduced shape.
- Similar observation for v_4

Non-linear responses

v4 comparison with eccentricity

